J. Fluid Mech. (2008), *vol.* 599, *pp.* 1–28.
doi:10.1017/S0022112007009640 Printed in the United Kingdom

Homogeneous turbulence in ferrofluids with a steady magnetic field

KRISTOPHER R. SCHUMACHER[1]†, JAMES J. RILEY[2] AND BRUCE A. FINLAYSON[1]

[1]Department of Chemical Engineering, University of Washington, Seattle, WA 98195, USA

[2]Department of Mechanical Engineering, University of Washington, Seattle, WA 98195, USA
kschuma@jhu.edu; rileyj@u.washington.edu; finlayson@cheme.washington.edu

(Received 1 May 2007 and in revised form 24 September 2007)

The general equations necessary for a basic theoretical interpretation of the physics of turbulence in ferrofluids are presented. The equations are examined and show multiple novel turbulence aspects that arise in ferrofluids. For example, two new modes of turbulent kinetic energy and turbulent kinetic energy dissipation rate occur, and unique modes of energy conversion (rotational to/from translational kinetic energy and magnetic energy to/from turbulent kinetic energy) are exhibited in turbulent ferrofluid flows. Furthermore, it is shown that potential models for turbulence in ferrofluids are complicated by additional closure requirements from the five additional nonlinear terms in the governing equations. The equations are applied to turbulence of a ferrofluid in the presence of a steady magnetic field (as well as the case of no magnetic field) in order to identify the importance of the new terms. Results are presented for the enhanced anisotropy in the presence of a magnetic field, and results show how turbulence properties (both classical ones and new ones) vary with the strength of the magnetic field. Three different equations for the magnetization are examined and lead to different results at large magnitudes of the applied magnetic field.

1. Introduction

A ferrofluid is a dielectric liquid with stable nanoscale (3–15 nm) magnetic particles suspended within it such that it responds strongly to magnetic fields. Each particle has a single magnetic domain with the magnetic dipole moment fixed rigidly within it. Brownian motion keeps the particles from settling in an external field, and an attached layer of surfactant helps prevent particle agglomeration through stearic hindrance. Ferrofluids should not be confused with magnetorheological fluids that have micron-sized magnetic particles and solidify or 'freeze up' in the presence of strong magnetic fields. Ferrofluids are stable and retain their ability to flow in intense magnetic fields. Ferrofluids are opaque and typically contain on the order of 10^{17} magnetic particles per cm^3 (Rosensweig 1985). They do not occur in nature and must be manufactured using either size reduction or chemical precipitation (Rosensweig 1985). Ferrofluids, sometimes called superparamagnetic liquids, have magnetic susceptibilities on the order of one, which is about three orders of magnitude larger than any other paramagnetic fluid (see table 1).

† Present address: Department of Biomedical Engineering, Johns Hopkins University, 720 Rutland Ave., 411 Traylor Building, Baltimore, MD 21205, USA.

Material	Susceptibility
Paramagnetic salt: $FeCl_3$	0.00046
Paramagnetic salt: $MnCl_2$	0.00090
Paramagnetic salt: $Ho(NO_3)_3$	0.00276
Typical ferrofluid	0.33

TABLE 1. Susceptibilities of some paramagnetic salts and a typical ferrofluid. The values for the salts are obtained from table 2.1 in Rosensweig (1985).

The ability to control and position ferrofluids using a magnetic force field leads to practical applications that include hermetic seals in pumps, computer hard drives and crystal growing apparatus. Ferrofluids exhibit convective effects in microgravity environments, and allow increased heat transfer in electrical devices on Earth due to magnetoconvection (Snyder, Cader & Finlayson 2003). There are also potential biomedical applications for concentrated drug delivery to specific target sites using external magnetic fields to guide the fluid or separate cells (Lübbe, Alexiou & Bergemann 2001; Roger *et al.* 1999; Ramchand *et al.* 2001; Berger *et al.* 2001).

The majority of ferrofluid studies are for stagnant or laminar flow cases. Experiments have shown that bulk ferrofluid flow can be induced with nothing more than a spatially uniform, rotating magnetic field (Moskowitz & Rosensweig 1967). In their system, magnetic body forces were zero, and fluid motion was driven by a microscopic torque mechanism. In some cases, Moskowitz & Rosensweig observed the formation of eddies in their torque-driven flow. In shear flows, the magnetic field can hinder free particle rotation, causing an additional resistance to flow to arise (McTague 1969). Laminar Poiseuille flow experiments in oscillating and rotating magnetic fields have shown fascinating results of drag reduction; for example, Poiseuille flow experiments with oscillating magnetic fields directed down the axis of the channel/pipe show that the effective viscosity can become lower than the viscosity in the absence of a magnetic field (Bacri *et al.* 1995; Zeuner, Richter & Rehberg 1998). It is interesting to note that Shliomis & Morozov (1994) predicted a decrease in effective viscosity using ferrofluid theory prior to experimental validation. Schumacher *et al.* (2003) and Krekhov, Shliomis & Kamiyama (2005) used the ferrofluid equations to predict the experimental results of Schumacher *et al.* (2003) for laminar flow in a pipe with an oscillating axial magnetic field.

Few studies of turbulent ferrofluid flow exist. Kamiyama (1996) studied the effects of a pressure drop in turbulent pipe flow in steady non-uniform transverse magnetic fields and found that increasing the magnitude of the magnetic field had little effect on the pressure drop. Schumacher *et al.* (2003) studied the pressure drop in turbulent pipe flow with uniform axially oscillating magnetic fields as a function of flow rate, magnetic field strength, and oscillation frequency. Pressure drop data showed a small dependence on magnetic field strength, but were almost independent of oscillation frequency and flow rate. Schumacher *et al.* (2003) showed that a k–ε turbulence model based on ferrofluid theory is capable of predicting the experimental turbulent pressure drop behaviour after an initial parameter fit to determine susceptibility dependence on the applied field. Anton (1990) measured velocity and turbulence intensities in the logarithmic region of a turbulent pipe flow with a non-uniform transverse magnetic field. Anton concluded that the magnetic field leads to suppression of turbulence.

In this paper we use direct numerical simulation (DNS) to study how the physics of turbulent flow is modified by the magnetic field and its interaction with a ferrofluid. In

a general sense, this is exploratory research on turbulence in fluids possessing internal angular momentum. The direct numerical simulation uses techniques that are standard in the field, but they are adapted to the complexities of the equations governing a ferrofluid, which are more numerous and have several additional nonlinear terms. Furthermore, ferrofluid phenomena involve time scales that are much smaller than for a Newtonian fluid.

The general equations that serve as a necessary framework for the interpretation of the physics of turbulence in ferrofluids are presented in § 2 along with the Reynolds stress and turbulent kinetic energy equations for ferrofluids. An emphasis is placed on the interpretation of the novel energy terms that arise due to ferrofluids. This section also presents several ways in which the magnetization can be modelled. The general turbulent kinetic energy equations are reduced for the specific case of homogeneous turbulence in § 3. Section 4 gives the physical parameters. Direct numerical simulation (§ 5) is used to study the energetics of forced turbulence in ferrofluids under the influence of an applied steady magnetic field, and the results are presented in § 6. The results of this study provide guidance on the relative importance of the new terms arising when a ferrofluid is in turbulent motion and, more generally, the results are important for developing reliable turbulence models for ferrofluids.

2. Governing equations

2.1. *Equations of motion*

The governing equations for ferrofluids are based on the theory of structured continua (Dahler & Scriven 1961, 1963), which allows fluids to have sub-continuum units with rotational degrees of freedom. The theory of structured continua augments the Cauchy equation for conservation of linear momentum,

$$\rho \mathrm{D}\boldsymbol{u}/\mathrm{D}t = \nabla \cdot \boldsymbol{T} + \rho \boldsymbol{S}, \tag{2.1}$$

with an equation of change for internal angular momentum,

$$\rho I \mathrm{D}\boldsymbol{\omega}/\mathrm{D}t = \nabla \cdot \boldsymbol{C} + \boldsymbol{Q} + \boldsymbol{A}, \tag{2.2}$$

where ρ is the density, $\boldsymbol{u}$ is the velocity, $\boldsymbol{\omega}$ is the ferrofluid particle spin rate, I is the moment of inertia of a ferrofluid particle, $\boldsymbol{T}$ is the stress tensor, $\boldsymbol{S}$ is the body force vector, $\boldsymbol{C}$ is the couple stress tensor, $\boldsymbol{Q}$ is the body couple per unit volume, and $\boldsymbol{A} = 2\zeta(\nabla \times \boldsymbol{u} - 2\boldsymbol{\omega})$ represents the production of internal angular momentum from external angular momentum, where the transfer coefficient ζ is called the vortex viscosity. Note that $\boldsymbol{A}/(4\zeta)$ represents the difference between the local fluid rotation rate ($\frac{1}{2}\nabla \times \boldsymbol{u}$) and the local ferrofluid particle rotation rate $\boldsymbol{\omega}$. A major result of this theory is that the external angular momentum (i.e. the moment of linear momentum) is no longer conserved. Thus, the usual arguments of stress tensor symmetry are no longer valid, and the viscous stress tensor has a symmetric and an asymmetric part, $\boldsymbol{T} = \boldsymbol{T}^s + \boldsymbol{T}^a$, where the superscripts s and a denote symmetric and asymmetric, respectively.

Rosensweig (1985) specialized the equations for a ferrofluid with the following constitutive relations. The symmetric part of the stress tensor is the usual expression for a Newtonian fluid, $\boldsymbol{T}^s = -p\boldsymbol{\delta} + 2\mu\boldsymbol{e} - \frac{2}{3}\mu(\nabla \cdot \boldsymbol{u})\boldsymbol{\delta}$, where μ is the dynamic viscosity, $\boldsymbol{e} = \frac{1}{2}(\nabla\boldsymbol{u} + \nabla\boldsymbol{u}^T)$ is the rate-of-strain tensor, p is the pressure and $\boldsymbol{\delta}$ is the unit tensor. The asymmetric stress tensor is written in terms of the vector $\boldsymbol{A}$, using the polyadic alternator epsilon, $\boldsymbol{T}^a = \frac{1}{2}\boldsymbol{\varepsilon} \cdot \boldsymbol{A}$, or, in index notation, $T^a_{ij} = \frac{1}{2}\varepsilon_{ijk}A_k$. The couple stress tensor is assumed symmetric and is taken to depend upon the angular spin rate

gradient, $\boldsymbol{C} = 2\eta'\boldsymbol{s}$, where $\boldsymbol{s} = \frac{1}{2}(\nabla\boldsymbol{\omega} + \nabla\boldsymbol{\omega}^T)$ is the spin-rate gradient tensor, and the transport coefficient η' is the spin viscosity. The magnetic body force is $\boldsymbol{S} = \mu_o \boldsymbol{M} \cdot \nabla \boldsymbol{H}$, and the magnetic body couple is $\boldsymbol{Q} = \mu_o \boldsymbol{M} \times \boldsymbol{H}$, where μ_o is the permeability of free space, $\boldsymbol{M}$ is the material magnetization vector, and $\boldsymbol{H}$ is the magnetic field vector. Substituting the constitutive equations into the linear momentum and internal angular momentum balances yields the governing equations of ferrofluid motion,

$$\rho\left(\frac{\partial \boldsymbol{u}}{\partial t} + \boldsymbol{u}\cdot\nabla\boldsymbol{u}\right) = -\nabla p + 2\mu\nabla\cdot\boldsymbol{e} + \zeta\nabla\times(2\boldsymbol{\omega} - \nabla\times\boldsymbol{u}) + \mu_o\boldsymbol{M}\cdot\nabla\boldsymbol{H}, \tag{2.3}$$

$$\rho I\left(\frac{\partial \boldsymbol{\omega}}{\partial t} + \boldsymbol{u}\cdot\nabla\boldsymbol{\omega}\right) = 2\eta'\nabla\cdot\boldsymbol{s} + 2\zeta(\nabla\times\boldsymbol{u} - 2\boldsymbol{\omega}) + \mu_o\boldsymbol{M}\times\boldsymbol{H}. \tag{2.4}$$

Ferrofluids are generally considered incompressible and with constant transport properties so that, in particular, the continuity equation is given by

$$\nabla\cdot\boldsymbol{u} = 0. \tag{2.5}$$

The governing equations, in index notation, are

$$\rho\frac{\partial u_i}{\partial t} + \rho u_k u_{i,k} = -p_{,i} + 2\mu e_{ij,j} - \frac{1}{2}\varepsilon_{ikl}A_{l,k} + S_i, \tag{2.6}$$

$$\rho I\left(\frac{\partial \omega_i}{\partial t} + u_k\omega_{i,k}\right) = \eta' s_{ij,j} + A_i + Q_i, \tag{2.7}$$

$$u_{k,k} = 0. \tag{2.8}$$

Note that because of $\boldsymbol{M}$ and $\boldsymbol{H}$, (2.3)–(2.5) do not form a closed set. Also, $\nabla\cdot\boldsymbol{\omega}$ is not necessarily zero, since the spin rate can differ significantly from the local fluid rotation rate, one-half the fluid vorticity. An additional equation that describes the changing material magnetization, along with Maxwell's equations for a non-conducting fluid, is necessary for closure. The various magnetization equations that have been proposed in the literature along with the use of Maxwell's equations are discussed below.

Vorticity is an important quantity in interpreting flow instabilities and turbulence. Therefore it is useful to examine how the vorticity equation for a ferrofluid is modified by the presence of a magnetic field and how the flow dynamics are changed. The curl of (2.3), using (2.5), gives the following equation for the vorticity $\boldsymbol{v} \equiv \nabla\times\boldsymbol{u}$:

$$\rho\frac{\mathrm{D}\boldsymbol{v}}{\mathrm{D}t} = (\boldsymbol{v}\cdot\nabla)\boldsymbol{u} + \mu\nabla^2\boldsymbol{v} - \tfrac{1}{2}\nabla\times(\nabla\times\boldsymbol{A}) + \mu_o\nabla\times(\boldsymbol{M}\cdot\nabla\boldsymbol{H}). \tag{2.9}$$

It is seen on the right-hand side that, in addition to the usual vortex stretching/turning and molecular diffusion terms that are present for a Newtonian fluid, there is also a term related to $\boldsymbol{A}$ and another to $\boldsymbol{M}$ and $\boldsymbol{H}$. Therefore, the local vorticity can be modified by differences between the local spin rate and local vorticity, and by the presence of gradients in the magnetic field. These influences can have important effects on the dynamics of a turbulent flow. Using vector identities, the term in (2.9) involving $\boldsymbol{A}$ can be written as

$$\begin{aligned} -\tfrac{1}{2}\nabla\times(\nabla\times\boldsymbol{A}) &= -\tfrac{1}{2}\nabla(\nabla\cdot\boldsymbol{A}) + \tfrac{1}{2}\nabla^2\boldsymbol{A} \\ &= -\tfrac{1}{2}\nabla(\nabla\cdot\boldsymbol{\omega}) + \tfrac{1}{2}\nabla^2\boldsymbol{A}, \end{aligned} \tag{2.10}$$

since $\nabla\cdot\boldsymbol{v} = \nabla\cdot(\nabla\times\boldsymbol{u}) = 0$. Therefore, the local vorticity is affected by local gradients of the divergence of the spin rate and by the Laplacian of the difference between the local spin rate and the local vorticity.

Under most conditions (see §4) the moment of inertia in the internal angular momentum equation is very small and the effect of the couple stress $\boldsymbol{C}$ is negligible. Then the spin equation, (2.4), becomes algebraic:

$$-\boldsymbol{A} = 2\zeta(2\boldsymbol{\omega} - \nabla \times \boldsymbol{u}) = \mu_o \boldsymbol{M} \times \boldsymbol{H} \quad \text{or} \quad \boldsymbol{\omega} = \frac{1}{2}\nabla \times \boldsymbol{u} + \frac{\mu_o}{4\zeta}\boldsymbol{M} \times \boldsymbol{H}. \tag{2.11}$$

and the spin can be eliminated from the magnetization equation (see (2.21), (2.24) and (2.26) discussed below), and from the momentum equation, (2.3):

$$\rho \frac{\partial \boldsymbol{u}}{\partial t} + \rho \boldsymbol{u} \cdot \nabla \boldsymbol{u} = -\nabla p + \mu \nabla^2 \boldsymbol{u} + \frac{\mu_o}{2}\nabla \times (\boldsymbol{M} \times \boldsymbol{H}) + \mu_o \boldsymbol{M} \cdot \nabla \boldsymbol{H}. \tag{2.12}$$

In that case, it can be shown (Shliomis 1972) that the entire theory can be represented by symmetric stresses without invoking an antisymmetric part or vortex viscosity. There is still a one-to-one correspondence between the parameters involving the vortex viscosity and the terms in the magnetization equation. Then the vortex viscosity is given by

$$\zeta = \frac{\mu_o \tau_B M_s^2}{6\chi}, \tag{2.13}$$

where τ_B is the Brownian time constant, χ is the magnetic susceptibility, and M_s is the saturation magnetization. Also note that replacing $\boldsymbol{A}$ by $-\mu_o \boldsymbol{M} \times \boldsymbol{H}$ in the third term on the right-hand side of (2.9), the vorticity equation, gives

$$-\tfrac{1}{2}\nabla \times (\nabla \times \boldsymbol{A}) = \tfrac{1}{2}\mu_o \nabla \times [\nabla \times (\boldsymbol{M} \times \boldsymbol{H})] = \tfrac{1}{2}\mu_o \nabla [\nabla \cdot (\boldsymbol{M} \times \boldsymbol{H})] - \tfrac{1}{2}\nabla^2 (\boldsymbol{M} \times \boldsymbol{H}). \tag{2.14}$$

2.2. *Energy equations*

Useful physical insights into a system can be obtained by considering how the primary components of energy are transported within the system. Therefore, the energy equations for ferrofluids are considered here. The terms in the equations, which represent the pathways of energy transfer between various energy components, are given an interpretation.

In ferrofluids, the kinetic energy consists of a translational component, $(\rho/2)u_i^2$, and a rotational component, $(\rho I/2)\omega_i^2$. The transport equations for the translational and rotational kinetic energies are derived in index notation, from (2.3) and (2.4) using (2.5). The internal energy equation for an incompressible fluid with no isotropic couple stress can be derived using a first law analysis (Brenner & Nadim 1996). The transport equations for translational kinetic energy, rotational kinetic energy, and internal energy are

$$\rho \frac{\mathrm{D}}{\mathrm{D}t}\frac{1}{2}u_i^2 = -(pu_j - 2\mu u_i e_{ij})_{,j} - 2\mu e_{ij} e_{ij} + \frac{1}{2}(\varepsilon_{ijk} u_j A_k)_{,j} - \frac{1}{4\zeta} A_i A_i - \omega_i A_i + \mu_o u_i M_j H_{i,j}, \tag{2.15}$$

$$\rho I \frac{\mathrm{D}}{\mathrm{D}t}\frac{1}{2}\omega_i^2 = 2\eta'(\omega_i s_{ij})_{,j} - 2\eta' s_{ij} s_{ij} + \omega_i A_i + \mu_0 \varepsilon_{ijk} \omega_i M_j H_k, \tag{2.16}$$

$$\rho \frac{\mathrm{D}\hat{U}}{\mathrm{D}t} = 2\mu e_{ij} e_{ij} + 2\eta' s_{ij} s_{ij} + \frac{1}{4\zeta} A_i A_i - q_{k,k} + \rho \hat{Q}_h, \tag{2.17}$$

where $\hat{U}$ is the internal energy per unit mass, q_k is the Fourier heat flux, and $\hat{Q}_h$ is a heat source. Note that the sum of the third, fourth, and fifth terms on the right-hand side of the translational kinetic energy equation is equivalent to $-(1/2)u_i \varepsilon_{ikl} A_{l,k}$,

according to the vector relationship:

$$-\frac{1}{2}\boldsymbol{u}\cdot(\nabla\times\boldsymbol{A})=\frac{1}{2}\nabla\cdot(\boldsymbol{u}\times\boldsymbol{A})-\frac{1}{4\zeta}\boldsymbol{A}\cdot\boldsymbol{A}-\boldsymbol{\omega}\cdot\boldsymbol{A}. \tag{2.18}$$

Consider the physical meaning of each of the terms on the right-hand side of (2.15)–(2.17). The first and third terms on the right-hand side of (2.15) represent the conservative rate of spatial transfer of translational kinetic energy due to pressure and viscous forces and the rate of spatial transfer of translational kinetic energy due to the presence of spin, respectively, while the last term represents the rate of work done on the system by the magnetic body force. The first term on the right-hand side of (2.16) represents the conservative rate of spatial transfer of rotational energy due to the spin viscosity, while the last term gives the rate of work done on the system by the magnetic body couple. The term, $2\mu e_{ij}e_{ij}$, represents the classical irreversible rate of transfer of translational kinetic energy into internal energy. Comparing (2.15) and (2.17), it is seen that $A_iA_i/(4\zeta)$ represents the irreversible transfer of translational kinetic energy to internal energy, due to the presence of spin. Comparing (2.15) and (2.16), it is seen that the term ω_iA_i gives the rate of transfer of translational kinetic energy from/to rotational kinetic energy. Comparing (2.16) and (2.17), it is seen that $2\eta's_{ij}s_{ij}$ represents the irreversible transfer of rotational kinetic energy into internal energy.

2.3. *Magnetization and Maxwell equations*

The momentum, spin, and continuity equations described above do not form a closed set, due to the $\boldsymbol{M}$ and $\boldsymbol{H}$ variables in the magnetic body force and body couple terms. Equations that describe the changing material magnetization, along with Maxwell's equations for a non-conducting fluid, are necessary for closure.

Maxwell's equations for a non-conducting fluid are

$$\nabla\cdot\boldsymbol{B}=0,\ \nabla\times\boldsymbol{H}=0. \tag{2.19a, b}$$

The magnetization is related to $\boldsymbol{B}$ and $\boldsymbol{H}$ using the definition

$$\boldsymbol{B}\equiv\mu_o(\boldsymbol{M}+\boldsymbol{H}). \tag{2.20}$$

The magnetic field $\boldsymbol{H}$ can be represented by a potential, $\boldsymbol{H}=\nabla\phi$, and Maxwell's equations are then satisfied with $\nabla^2\phi=-\nabla\cdot\boldsymbol{M}$.

At least three different magnetization equations, which are described below, have been proposed in the literature. The first, and original, ferrofluid magnetization equation was proposed by Shliomis (1972). A second magnetization equation, proposed by Martsenyuk, Raikher & Shliomis (1974), was derived from the Fokker–Planck equation using the effective field method. The third equation, proposed by Felderhof & Kroh (1999), was derived based on irreversible thermodynamics.

The magnetization equation proposed by Shliomis (1972) is

$$\frac{\partial\boldsymbol{M}}{\partial t}=-\boldsymbol{u}\cdot\nabla\boldsymbol{M}+\boldsymbol{\omega}\times\boldsymbol{M}-\frac{1}{\tau}(\boldsymbol{M}-\boldsymbol{M}_0), \tag{2.21}$$

where τ is the relaxation time of the ferrofluid particles (defined in §4) and $\boldsymbol{M}_0$ is the equilibrium magnetization. The equilibrium magnetization is determined by the magnetic equation of state,

$$\boldsymbol{M}_0=M_SL(\xi)\frac{\boldsymbol{H}}{H}, \tag{2.22}$$

where

$$L(\xi) = \frac{1}{\tanh(\xi)} - \frac{1}{\xi}, \quad \xi = \frac{\mu_o m H}{k_B T}, \quad H = \sqrt{H_x^2 + H_y^2 + H_z^2}. \tag{2.23a–c}$$

Here M_S is the saturation magnetization, m is the magnetic moment of a single particle, and k_B is Boltzmann's constant.

The magnetization equation derived by Felderhof & Kroh (1999) is

$$\frac{\partial \boldsymbol{M}}{\partial t} = -\boldsymbol{u}\cdot\nabla\boldsymbol{M} + \boldsymbol{\omega}\times\boldsymbol{M} - \frac{\chi_o}{\tau}[\boldsymbol{H} - \boldsymbol{H}_{eq}], \tag{2.24}$$

where χ_o is the initial magnetic susceptibility, and $\boldsymbol{H}_{eq}$ is the local equilibrium magnetic field. Here the initial susceptibility is $\chi_o = \lim_{H\to 0}(M_0/H) = (\mu_o m M_S)/(3k_B T)$. The local equilibrium magnetic field is $\boldsymbol{H}_{eq} = \boldsymbol{M}C(M)$, where the following equation is solved for C, given M:

$$C^{-1} = \frac{M_S}{MC}\left\{\left(\tanh\left(\frac{3\chi_o}{M_S}MC\right)\right)^{-1} - \left(\frac{3\chi_o}{M_S}MC\right)^{-1}\right\}, \quad M = \sqrt{M_x^2 + M_y^2 + M_z^2}. \tag{2.25a, b}$$

The magnetization equation proposed by Martsenyuk *et al.* (1974) is

$$\frac{\partial \boldsymbol{M}}{\partial t} = -\boldsymbol{u}\cdot\nabla\boldsymbol{M} + \left(\frac{1}{2}\nabla\times\boldsymbol{u}\right)\times\boldsymbol{M} - \frac{3\chi_o}{2\tau M^2}\left(1 - \frac{3L(\xi_e)}{\xi_e}\right)\boldsymbol{M}\times(\boldsymbol{M}\times\boldsymbol{H}) - \frac{1}{\tau}\left[\boldsymbol{M} - \frac{3\chi_o L(\xi_e)}{\xi_e}\boldsymbol{H}\right]. \tag{2.26}$$

ξ_{ei} is the non-dimensional effective magnetic field for which the non-equilibrium magnetization, M_i, is an equilibrium magnetization. The effective field is related to M_i by the equation

$$M_i = M_S L(\xi_e)\frac{\xi_{ei}}{\xi_e}, \tag{2.27}$$

where

$$\xi_{ei} = \frac{\mu_o m H_{ei}}{k_B T}. \tag{2.28}$$

2.4. *Averaged equations*

To obtain the Reynolds-averaged equations, we use a Reynolds decomposition to write each dependent variable (u_j, p, ω_i, M_i, H_i) as the sum of a mean and fluctuating component, e.g. for velocity, $u_i = \overline{u}_i + u_i'$, where an overbar represents the mean component and the prime designates the fluctuating component. We substitute the decomposed variables into the governing equations and subsequently average each term to get the mean linear momentum

$$\rho\frac{\partial \overline{u}_i}{\partial t} + \rho\overline{u}_k\overline{u}_{i,k} = -\overline{p}_{,i} + 2\mu\overline{e}_{ik,k} - \rho(\overline{u_k' u_i'})_{,k} - \tfrac{1}{2}\varepsilon_{ikl}\overline{A}_{l,k} + \overline{S}_i, \tag{2.29}$$

the mean internal angular momentum

$$\rho I\frac{\partial \overline{\omega_i}}{\partial t} + \rho I\overline{u}_k\overline{\omega}_{i,k} = 2\eta'\overline{s}_{ik,k} + \overline{A}_i + \overline{Q}_i - \rho I\overline{u_k'\omega_{i,k}'} \tag{2.30}$$

and the mean continuity

$$\overline{u}_{k,k} = 0, \tag{2.31}$$

where

$$\overline{A}_i = 2\zeta(\varepsilon_{ikl}\overline{u}_{l,k} - 2\overline{\omega}_i), \tag{2.32a}$$

$$\overline{S}_i = \mu_o \overline{M}_k \overline{H}_{i,k} + \mu_o \overline{M'_k H'_{i,k}}, \tag{2.32b}$$

$$\overline{Q}_i = \mu_o \varepsilon_{ikl} \overline{M}_k \overline{H}_l + \mu_o \varepsilon_{ikl} \overline{M'_k H'_l}. \tag{2.32c}$$

The left-hand side and the first three terms on the right-hand side of (2.29) are the same as the mean flow equation for a Newtonian fluid (see e.g. McComb 1992; Pope 2000). The Reynolds stress term, $-\rho\overline{u'_k u'_i}$, causes the well-known 'turbulence closure problem', and is interpreted as spatial flux of mean momentum due to the turbulence. Great effort has been invested in deriving appropriate models for the Reynolds stress term. In ferrofluids, there are three additional nonlinear terms in (2.29) and (2.30) $\overline{u'_k\omega'_{i,k}}$, $\overline{M'_k H'_{i,k}}$, and $\overline{M'_k H'_l}$. Note that $\overline{u'_k\omega'_{i,k}} = (\overline{u'_k\omega'_i})_{,k}$ since $u'_{k,k} = 0$ from (2.5) and (2.31). The correlation $\overline{u'_k\omega'_i}$ can be interpreted as the flux of mean internal angular momentum by the turbulence, analogous to the Reynolds stress. The terms $\overline{M'_k H'_{i,k}}$ and $\overline{M'_k H'_i}$ indicate the effect of magnetic field fluctuations on the mean flow. Thus, the turbulence closure problem is more complex for ferrofluids. In addition to these new terms which require modelling, it would be expected that terms such as the Reynolds stresses would require new modelling, as the magnetic field modifies the physics of the turbulent flow.

Note that when the moment of inertia and couple stress terms are neglected in the angular momentum equations, the averaged angular momentum equation reduces to

$$\overline{\omega}_i = \frac{1}{2}\varepsilon_{ikl}\overline{u}_{l,k} + \frac{\mu_o}{4\zeta}(\varepsilon_{ikl}\overline{M}_k\overline{H}_l + \varepsilon_{ikl}\overline{M'_k H'_l}). \tag{2.33}$$

2.5. *Reynolds stress equations*

To obtain the equations for Reynolds stresses and related quantities, first the transport equations for the fluctuating components of velocity and spin are derived by subtracting their respective mean equations from the Reynolds-decomposed equations. Next, each term in the fluctuating equation for velocity u'_i is multiplied by u'_j, then another equation is written by interchanging the subscripts i and j, the two equations are added together and then each term is averaged. The result is the Reynolds stress equation:

$$\begin{aligned}\frac{\partial\overline{u'_i u'_j}}{\partial t} + \overline{u}_k(\overline{u'_i u'_j})_{,k} = &-[\overline{u'_i u'_k}\,\overline{u}_{j,k} + \overline{u'_j u'_k}\,\overline{u}_{i,k}] - [(\overline{u'_i u'_j u'_k}) + \tfrac{1}{\rho}(\overline{u'_j p'})\delta_{ik} + \tfrac{1}{\rho}(\overline{u'_i p'})\delta_{jk} \\ &+ \nu(\overline{u'_i u'_j})_{,k}]_{,k} + \tfrac{1}{\rho}[\overline{p'(u'_{i,j} + u'_{j,i})}] - 2\nu\overline{u'_{i,k}u'_{j,k}} - \tfrac{1}{2\rho}[\overline{u'_j\varepsilon_{ikl}A'_{l,k}} + \overline{u'_i\varepsilon_{jkl}A'_{l,k}}] \\ &+ \tfrac{1}{\rho}[\overline{u'_j S'_i} + \overline{u'_i S'_j}].\end{aligned} \tag{2.34}$$

The first square-bracketed terms on the right-hand side represent the production tensor, the second square-bracketed terms are the turbulent and molecular transport terms, the next term is the pressure/rate-of-strain tensor, and the following term is the dissipation-rate tensor. The new terms are the last two sets of square-bracketed terms. The first represents the correlation of the velocity with the curl of the vector $\boldsymbol{A}$, i.e. with the divergence of the asymmetric component of the stress tensor, while the last represents the correlation between the velocity and the magnetic body force.

The analogous correlation equation for the fluctuating spin is

$$\rho I\left(\frac{\partial\overline{\omega_i'\omega_j'}}{\partial t}+\overline{u}_k(\overline{\omega_i'\omega_j'})_{,k}\right)=-\rho I\left[(\overline{\omega_j'u_k'}\;\overline{\omega}_{i,k}+\overline{\omega_i'u_k'}\;\overline{\omega}_{j,k})\right]-\rho I\overline{u_k'(\omega_i'\omega_j')_{,k}}$$
$$+\eta'(\overline{\omega_j'\omega_i'})_{,kk}-2\eta'\overline{\omega_{i,k}'\omega_{j,k}'}+\left[\overline{\omega_j'A_i'}+\overline{\omega_i'A_j'}\right]+\left[\overline{\omega_j'Q_i'}+\overline{\omega_i'Q_j'}\right]. \quad (2.35)$$

The first bracketed term on the right-hand side is the production term; the second is a turbulent diffusion term; the third term is a molecular diffusion term; and the fourth term is the dissipation rate term. The last two sets of bracketed terms represent the correlations of spin with the asymmetric component of the stress tensor and the magnetic body torque, respectively. An equation for $\overline{\omega_j'u_i'}$, the flux of mean internal angular momentum identified above, can be derived by multiplying the u_i' equation by $I\omega_j'$, then multiplying the $I\omega_i'$ equation by u_j', adding, taking the average, and dividing by ρI. When the spin viscosity is zero and the moment of inertia is small (both assumptions are justified in § 4), this equation reduces to

$$\overline{u_j'A_i'}+\overline{u_i'A_j'}+\overline{u_j'Q_i'}+\overline{u_i'Q_j'}=0. \quad (2.36)$$

2.6. *Turbulent energy equations*

The mean kinetic energy is an important quantity in turbulent flows. Here, we use Reynolds decomposition to expand the mean energies. Then, the transport equations for the turbulent kinetic energy, which are an important tool in the subsequent analysis of how the energetics of turbulent flow is modified for ferrofluids, are developed and the terms in the equations are interpreted.

The mean translational kinetic energy is composed of a mean velocity term and a fluctuating velocity term, and is given by $(\rho/2)\,\overline{u_i^2}=(\rho/2)\,\overline{u}_i^2+(\rho/2)\,\overline{u_i'^2}$. The term $(\rho/2)\,\overline{u_i'^2}$ is the translational turbulent kinetic energy; in Newtonian flows, this term is often called the turbulent kinetic energy. Similarly, the mean rotational kinetic energy is composed of a mean spin term and a fluctuating spin term, and is given by $(\rho I/2)\,\overline{\omega_i^2}=(\rho I/2)\,\overline{\omega}_i^2+(\rho I/2)\,\overline{\omega_i'^2}$. The term $(\rho I/2)\,\overline{\omega_i'^2}$ represents the rotational turbulent kinetic energy.

The transport equations for the turbulent kinetic energies are obtained by setting the subscripts in the Reynolds stress and fluctuating spin equations equal to each other ($i=j$), with then an implied summation on i, and multiplying through by $1/2$. The results are

$$\rho\tfrac{\partial}{\partial t}\tfrac{1}{2}\overline{u_i'^2}+\rho\overline{u}_k\left[\tfrac{1}{2}\overline{u_i'^2}\right]_{,k}=-\left[\rho\overline{u_k'\tfrac{1}{2}u_i'^2}-(\overline{p'u_k'})\delta_{ik}-2\mu\overline{u_i'e_{ik}'}\right]_{,k}-\rho\overline{u}_{i,j}\overline{u_i'u_j'}$$
$$-2\mu\overline{e_{ij}'e_{ij}'}+\tfrac{1}{2}(\varepsilon_{ijk}\overline{u_j'A_k'})_{,i}-\tfrac{1}{4\zeta}\overline{A_i'A_i'}-\overline{\omega_i'A_i'}$$
$$+\mu_0\left[\overline{M}_j\overline{u_i'H_{i,j}'}+\overline{u_i'M_j'}\overline{H}_{i,j}+\overline{u_i'M_j'H_{i,j}'}\right], \quad (2.37)$$

$$\rho I\tfrac{\partial}{\partial t}\tfrac{1}{2}\overline{\omega_i'^2}+\rho I\overline{u}_k\left[\tfrac{1}{2}\overline{\omega_i'^2}\right]_{,k}=-\left[\rho I\,\overline{u_k'\tfrac{1}{2}\omega_i'^2}-2\eta'\overline{\omega_i's_{ik}'}\right]_{,k}-2\eta'\overline{s_{ij}'s_{ij}'}+\overline{\omega_i'A_i'}$$
$$+\mu_o\varepsilon_{ijk}[\overline{\omega_i'M_j'}\overline{H}_k+\overline{M}_j\overline{\omega_i'H_k'}+\overline{\omega_i'M_j'H_k'}]. \quad (2.38)$$

Note that in (2.37) the first square-bracketed terms on the right-hand side represent the rates of turbulent and molecular transport of translational turbulent kinetic energy, the second term is the rate of production term from the mean velocity field, and the third term is the classical dissipation rate of translational turbulent kinetic energy. The fourth term represents the rate of turbulent diffusion of translational turbulent kinetic energy by fluctuations in $\boldsymbol{A}$, the fifth term is the dissipation rate of turbulent kinetic energy due to the fluctuations in $\boldsymbol{A}$, the sixth term represents the

transfer rate of translational turbulent kinetic energy to/from rotational turbulent kinetic energy, and the last bracketed terms represent the rate of work done on the turbulence due to fluctuations in $\boldsymbol{u}$, $\boldsymbol{M}$, and $\boldsymbol{H}$. In (2.38) for the turbulent rotational kinetic energy, the first square-bracketed terms on the right-hand side represent the rates of turbulent and molecular transport of the turbulent rotational kinetic energy, the second term is the dissipation rate of rotational kinetic energy into internal energy, the third represents the transfer rate of turbulent rotational kinetic energy from/to turbulent kinetic energy, while the last bracketed terms represent the rate of work done on the system due to fluctuations in $\boldsymbol{\omega}$, $\boldsymbol{M}$, and $\boldsymbol{H}$. Finally, we complete the set of averaged energy equations by averaging the internal energy equation, giving

$$\rho\frac{\partial\overline{\hat{U}}}{\partial t}+\rho\hat{u}_k(\overline{\hat{U}})_{,k}=2\mu\bar{e}_{ij}\bar{e}_{ij}+2\mu\overline{e'_{ij}e'_{ij}}+2\eta'\bar{s}_{ij}\bar{s}_{ij}+2\eta'\overline{s'_{ij}s'_{ij}}+\frac{1}{4\zeta}\overline{A}_i\overline{A}_i+\frac{1}{4\zeta}\overline{A'_iA'_i}-\overline{q}_{k,k}+\rho\,\overline{\hat{Q}}_h. \tag{2.39}$$

In (2.39), the first two terms on the right-hand side represent the molecular dissipation rates of mean flow and turbulent kinetic energies into mean internal energy, respectively, while the third and fourth terms represent the molecular dissipation rates of mean flow and turbulent rotational kinetic energies into mean internal energy. The fifth and sixth terms represent the dissipation rates of mean flow and turbulent kinetic energies into mean internal energy due to the presence of spin.

2.7. *Turbulent magnetic equations*

The fields of $\boldsymbol{B}$, $\boldsymbol{M}$, and $\boldsymbol{H}$ can be decomposed into mean and fluctuating components:

$$\boldsymbol{B}=\overline{\boldsymbol{B}}+\boldsymbol{B}',\quad \boldsymbol{M}=\overline{\boldsymbol{M}}+\boldsymbol{M}',\quad \boldsymbol{H}=\overline{\boldsymbol{H}}+\boldsymbol{H}', \tag{2.40a–c}$$

so that Maxwell's equations for a non-conducting medium can be separated into mean and fluctuating parts as well:

$$\nabla\cdot\overline{\boldsymbol{B}}=0,\quad \nabla\times\overline{H}=0,\quad \overline{\boldsymbol{H}}=\nabla\overline{\phi},\quad \nabla^2\overline{\phi}=-\nabla\cdot\overline{\boldsymbol{M}}, \tag{2.41a–d}$$

$$\nabla\cdot\boldsymbol{B}'=0,\quad \nabla\times H'=0,\quad \boldsymbol{H}'=\nabla\phi',\quad \nabla^2\phi'=-\nabla\cdot\boldsymbol{M}'. \tag{2.42a–d}$$

It is useful to examine some of the issues that arise in dealing with the equation for the average of $\boldsymbol{M}$. For example, averaging the simplest equation for $\boldsymbol{M}$, (2.21), gives

$$\frac{\partial\overline{\boldsymbol{M}}}{\partial t}+\overline{\boldsymbol{u}}\cdot\nabla\overline{\boldsymbol{M}}=-\nabla\cdot\overline{\boldsymbol{u}'\boldsymbol{M}'}+\overline{\boldsymbol{\omega}}\times\overline{\boldsymbol{M}}+\overline{\boldsymbol{\omega}'\times\boldsymbol{M}'}-\frac{1}{\tau}(\overline{\boldsymbol{M}}-\overline{\boldsymbol{M}}_0). \tag{2.43}$$

Terms requiring modelling are the following. The first term on the right-hand side, $-\nabla\cdot\overline{\boldsymbol{u}'\boldsymbol{M}'}$, represents the divergence of the turbulent flux of $\overline{\boldsymbol{M}}$, and probably requires modelling similar to that of the turbulent flux of other quantities. The third term, $\overline{\boldsymbol{\omega}'\times\boldsymbol{M}'}$, involves the correlation of the fluctuations in $\boldsymbol{\omega}$ and $\boldsymbol{M}$. The term, $\overline{\boldsymbol{M}}_0$, involving the average of the equilibrium magnetization, involves the average of a complicated function of the magnitude of the magnetic field $\boldsymbol{H}$ (see equation (2.22)). This may be difficult to model by standard methods, and may require information about the probability density of $\boldsymbol{H}$, so that the model might then require at least the first two moments of $\boldsymbol{H}$. Note that if $\xi=(\mu_o mH)/(k_BT)$ is 'small', then $L(\xi)=1/\tanh(\xi)-1/\xi\approx\xi/3+O(\xi^3)$, and to lowest order, $\boldsymbol{M}_0=((\mu_o mM_s)/(3k_BT))\,\boldsymbol{H}$. Therefore, to lowest order, $\overline{\boldsymbol{M}}_0((\mu_o mM_s)/(3k_BT))\overline{\boldsymbol{H}}$.

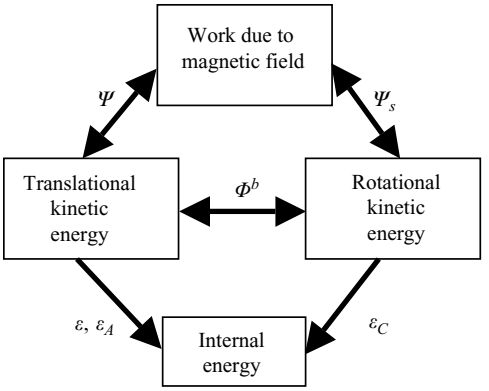

FIGURE 1. Energy modes diagram for a ferrofluid system.

3. Homogeneous ferrofluid turbulence equations

Consider the turbulent flow of a ferrofluid that is assumed to be statistically homogeneous and contained within a cube, with periodic boundary conditions, of volume V and side length, L. Assume that L is large relative to the integral length scale of the flow, $\mathscr{L}$. Assume that the fluid is isothermal, there are no external heat effects, and that the mean velocity and spin gradients are zero, such that $\overline{e}_{ij} = \overline{s}_{ij} = 0$.

First, we reduce the general turbulent kinetic energy equations for the specific case of homogeneous turbulence. In this case, the spatial gradients of all averaged quantities are zero, so that the averaged turbulent energy equations, (2.37)–(2.39), become

$$\frac{\mathrm{d}E_t}{\mathrm{d}t} = -\varepsilon - \varepsilon_A - \Phi^b + \Psi, \tag{3.1}$$

$$\frac{\mathrm{d}E_r}{\mathrm{d}t} = -\varepsilon_C + \Phi^b + \Psi_s, \tag{3.2}$$

$$\frac{\mathrm{d}U}{\mathrm{d}t} = \varepsilon + \varepsilon_A + \varepsilon_C, \tag{3.3}$$

where

$$E_t = \tfrac{1}{2}\rho\overline{u_i'^2}, \quad E_r = \tfrac{1}{2}\rho I\overline{\omega_i'^2}, \quad U = \rho\overline{\hat{U}}, \quad \varepsilon = 2\mu\overline{e_{ij}'e_{ij}'}, \tag{3.4a–d}$$

$$\varepsilon_A = \frac{1}{4\zeta}\overline{A_i'A_i'}, \quad \varepsilon_C = 2\eta'\overline{s_{ij}'s_{ij}'}, \quad \Phi^b = \overline{\omega_i'A_i'}, \quad \Psi = \overline{u_i'S_i'}, \quad \Psi_s = \overline{\omega_i'Q_i'}. \tag{3.4e–i}$$

As discussed in § 5, there are several terms representing the transfer rates of one form of energy to another. ε is the classical viscous dissipation rate of translational turbulent kinetic energy due to viscous shear stresses, ε_C is the dissipative rate of loss of rotational kinetic energy due to couple stresses $\boldsymbol{C}$, Φ^b is the rate of work done on the spin by asymmetric stresses, and results in the transfer of translational kinetic energy to/from rotational kinetic energy, ε_A is the dissipation rate of translational kinetic energy due to the antisymmetric part of the stress ($\boldsymbol{A}$), Ψ is considered to be the rate of work done on the turbulent flow by magnetic body forces, and Ψ_s is the rate of work done on the turbulent flow by magnetic body couples. The terms ε_A, ε_C, Φ^b, Ψ, Ψ_s are novel to ferrofluids, and if these terms are zero, the turbulent energy equations become the same as those of a Newtonian fluid.

The turbulent energy transfer modes are illustrated in figure 1. The dissipative terms, ε, ε_A, and ε_C, are each non-negative, and act as sink terms for turbulent kinetic energies. The transfer term between translational turbulent kinetic energy and rotational turbulent kinetic energy, Φ^b, is positive or negative depending on whether

the spin rate is slower or faster than the local fluid rotation rate. Thus, rotational turbulent kinetic energy can be transferred to translational turbulent kinetic energy (when Φ^b is negative). The transfer terms, Ψ and Ψ_s, represent turbulent energy transfer due to the magnetic terms in the equation, and they can act as a source or sink for energy within the system. Thus, energy can be injected into the flow by means of the magnetic forces, and this energy can affect the translational turbulent kinetic energy, rotational turbulent kinetic energy, and ultimately the internal energy.

Then it is convenient to expand the dependent variables in Fourier series, where here a caret denotes the Fourier transform, i.e.

$$u_i(\boldsymbol{x}) = \sum_{\boldsymbol{k}} \hat{u}_i(\boldsymbol{k}) \mathrm{e}^{\mathrm{i}\boldsymbol{k}\cdot\boldsymbol{x}}, \quad \hat{u}_i(\boldsymbol{k}) = \frac{1}{L^3}\int_{-L/2}^{L/2} u_i(\boldsymbol{x}) \mathrm{e}^{-\mathrm{i}\boldsymbol{k}\cdot\boldsymbol{x}}\,\mathrm{d}\boldsymbol{x}, \tag{3.4a, b}$$

where $\boldsymbol{k} = ((2\pi)/L)\,\boldsymbol{n}$, and $\boldsymbol{n}$ has components $n_1, n_2, n_3 = 0, \pm 1, \pm 2, \ldots$. The ferrofluid momentum equation in Fourier space is

$$\frac{\mathrm{d}\hat{u}_i(\boldsymbol{k})}{\mathrm{d}t} = \hat{\tau}_i(\boldsymbol{k}) + \hat{\alpha}_i(\boldsymbol{k}) + \hat{\psi}_i(\boldsymbol{k}) - \nu k^2 \hat{u}_i(\boldsymbol{k}), \tag{3.5}$$

where

$$\hat{\tau}_i = \left(\delta_{ij} - \frac{k_i k_j}{k^2}\right)\hat{F}_j^{(1)}(\boldsymbol{k}), \quad \hat{\alpha}_i = \left(\delta_{ij} - \frac{k_i k_j}{k^2}\right)\hat{F}_j^{(2)}(\boldsymbol{k}), \tag{3.6a, b}$$

$$\hat{\psi}_i = \left(\delta_{ij} - \frac{k_i k_j}{k^2}\right)\hat{F}_j^{(3)}(\boldsymbol{k}), \quad F_j^{(1)} = \{\boldsymbol{u} \times (\nabla \times \boldsymbol{u})\}, \tag{3.6c, d}$$

$$F_j^{(2)} = \left\{\frac{\zeta}{\rho}\nabla \times (2\boldsymbol{\omega} - \nabla \times \boldsymbol{u})\right\}_j, \quad F_j^{(3)} = \left\{\frac{\mu_o}{\rho}\boldsymbol{M}\cdot\nabla\boldsymbol{H}\right\}_j. \tag{3.6e, f}$$

The Fourier transform of the continuity equation is

$$\boldsymbol{k}\cdot\hat{\boldsymbol{u}}(\boldsymbol{k}) = 0. \tag{3.7}$$

The Fourier transform of the spin equation is

$$\frac{\partial(I\hat{\omega}_i(\boldsymbol{k}))}{\partial t} = -\hat{\gamma}_i(\boldsymbol{k}) + \frac{1}{\rho}\hat{A}_i(\boldsymbol{k}) + \frac{\mu_o}{\rho}\hat{Q}_i(\boldsymbol{k}) - \frac{\eta'}{\rho}k^2\hat{\omega}_i(\boldsymbol{k}) \tag{3.8}$$

where

$$\gamma_i = I u_j \omega_{i,j}, \quad \hat{\boldsymbol{A}} = 2\zeta(\mathrm{i}\boldsymbol{k}\times\hat{\boldsymbol{u}} - 2\hat{\boldsymbol{\omega}}), \quad Q = \boldsymbol{M}\times\boldsymbol{H}. \tag{3.9a–c}$$

Spectral analysis is a useful tool to gain insight into the distribution of energy in wavenumber space. In order to analyse the transfer of energy between different wavenumber modes, we derive the Fourier space form of the translational turbulent kinetic energy equation. This is achieved by first multiplying (3.5) by $\hat{u}_i^*(\boldsymbol{k})$, then multiply each term in the complex conjugate form of (3.5) by $\hat{u}_i(\boldsymbol{k})$, summing the two equations, and averaging (e.g. see Pope, 2000)

$$\frac{\mathrm{d}\hat{E}_t(\boldsymbol{k})}{\mathrm{d}t} = \hat{T}(\boldsymbol{k}) + \hat{\Phi}^a(\boldsymbol{k}) + \hat{\Psi}(\boldsymbol{k}) - \hat{\varepsilon}(\boldsymbol{k}), \tag{3.10}$$

where

$$\hat{E}_t(\boldsymbol{k}) = \tfrac{1}{2}\langle\hat{u}_i(\boldsymbol{k})\hat{u}_i^*(\boldsymbol{k})\rangle, \quad \hat{T}(\boldsymbol{k}) = \tfrac{1}{2}[\langle\hat{u}_i(\boldsymbol{k})\hat{\tau}_i^*(\boldsymbol{k})\rangle + \langle\hat{u}_i^*(\boldsymbol{k})\hat{\tau}_i(\boldsymbol{k})\rangle], \tag{3.11a, b}$$

$$\hat{\Phi}^a(\boldsymbol{k}) = \tfrac{1}{2}[\langle\hat{u}_i(\boldsymbol{k})\hat{\alpha}_i^*(\boldsymbol{k})\rangle + \langle\hat{u}_i^*(\boldsymbol{k})\hat{\alpha}_i(\boldsymbol{k})\rangle], \tag{3.11c}$$

$$\hat{\Psi}(\boldsymbol{k}) = \tfrac{1}{2}[\langle\hat{u}_i(\boldsymbol{k})\hat{\psi}_i^*(\boldsymbol{k})\rangle + \langle\hat{u}_i^*(\boldsymbol{k})\hat{\psi}_i(\boldsymbol{k})], \quad \hat{\varepsilon}(\boldsymbol{k}) = \nu k^2\langle\hat{u}_i(\boldsymbol{k})\hat{u}_i^*(\boldsymbol{k})\rangle. \tag{3.11d, e}$$

Here $\langle \cdot \rangle$ represents the averaging operator in the spectral domain. The rotational turbulent kinetic energy equation in Fourier space, derived in an analogous manner, is

$$\frac{\mathrm{d}\hat{E}_r(\boldsymbol{k})}{\mathrm{d}t} = \hat{\Gamma}(\boldsymbol{k}) + \hat{\Phi}^b(\boldsymbol{k}) + \hat{\Psi}_s(\boldsymbol{k}) - \hat{\varepsilon}_C(\boldsymbol{k}) \tag{3.12}$$

where

$$\hat{E}_r(\boldsymbol{k}) = \tfrac{1}{2} I \langle \hat{\omega}_i(\boldsymbol{k}) \hat{\omega}_i^*(\boldsymbol{k}) \rangle, \quad \hat{\Gamma}(\boldsymbol{k}) = \tfrac{1}{2} I [\langle \hat{\omega}_i^*(\boldsymbol{k}) \hat{\gamma}_i(\boldsymbol{k}) + \hat{\omega}_i(\boldsymbol{k}) \hat{\gamma}_i^*(\boldsymbol{k}) \rangle] \tag{3.13a, b}$$

$$\rho \hat{\Phi}^b = \tfrac{1}{2} [\langle \hat{\omega}_i^*(\boldsymbol{k}) \hat{A}_i \rangle + \langle \hat{\omega}_i(\boldsymbol{k}) \hat{A}_i^* \rangle], \tag{3.13c}$$

$$\rho \hat{\Psi}_s(\boldsymbol{k}) = \mu_o / 2 [\langle \hat{\omega}_i^*(\boldsymbol{k}) \hat{Q}_i \rangle + \langle \hat{\omega}_i(\boldsymbol{k}) \hat{Q}_i^* \rangle], \quad \rho \hat{\varepsilon}_C(\boldsymbol{k}) = \eta' k^2 \langle \hat{\omega}_i(\boldsymbol{k}) \hat{\omega}_i^*(\boldsymbol{k}) \rangle. \tag{3.13d, e}$$

Equation (3.10) describes how the wavenumber distribution of turbulent kinetic energy changes with time. $\hat{E}_t$ is the spectrum of translational turbulent kinetic energy, $\hat{T}$ is the spectrum of the inertial transfer rate of the translational turbulent kinetic energy, and $\hat{\varepsilon}$ is the spectrum of the classical viscous dissipation rate of translational turbulent kinetic energy due to viscous shear stresses. $\hat{\Phi}^a$ is interpreted to be the spectrum of work done on the vorticity by asymmetric stresses, and contains both the transform of the dissipation rate of translational kinetic energy, $\hat{\varepsilon}_A$, and the transform of the transfer rate between translation and rotational kinetic energies, $\hat{\Phi}^b$ (see also equation (2.31)). $\hat{\Psi}$ can be considered to be the spectrum of energy conversion between kinetic and magnetic degrees of freedom. In a Newtonian fluid, $\hat{\Phi}^a$ and $\hat{\Psi}$ are zero.

Equation (3.12) describes how the wavenumber distribution of turbulent translational kinetic energy changes with time. Here, $\hat{E}_r$ is the spectrum of rotational turbulent kinetic energy of the rotating particles, $\hat{\Gamma}$ is the spectrum of the inertial transfer rate of the rotational turbulent kinetic energy (analogous to $\hat{T}$), $\hat{\Phi}^b$ is the spectrum of the exchange terms mentioned above, $\hat{\Psi}_s$ is the spectrum of energy conversion between rotational and magnetic degrees of freedom, and $\hat{\varepsilon}_C$ is the spectrum of the rate of dissipative loss of rotational turbulent kinetic energy due to couple stresses.

Note that the transform of the dissipation rate of translational turbulent kinetic energy due to A_i can be expressed as $\hat{\varepsilon}_A(\boldsymbol{k}) = -\hat{\Phi}^a(\boldsymbol{k}) - \hat{\Phi}^b(k)$. This expression can be used to rewrite the kinetic, rotational, and internal energy spectrum equations as

$$\frac{\mathrm{d}\hat{E}_t(\boldsymbol{k})}{\mathrm{d}t} = \hat{T}(\boldsymbol{k}) - \hat{\varepsilon}_A(\boldsymbol{k}) - \hat{\Phi}^b(\boldsymbol{k}) + \hat{\Psi}(\boldsymbol{k}) - \hat{\varepsilon}(\boldsymbol{k}), \tag{3.14}$$

$$\frac{\mathrm{d}\hat{E}_r(\boldsymbol{k})}{\mathrm{d}t} = \hat{\Gamma}(\boldsymbol{k}) + \hat{\Phi}^b(\boldsymbol{k}) + \hat{\Psi}_s(\boldsymbol{k}) - \hat{\varepsilon}_C(\boldsymbol{k}), \tag{3.15}$$

$$\frac{\mathrm{d}\hat{U}_s(\boldsymbol{k})}{\mathrm{d}t} = \hat{\varepsilon}(\boldsymbol{k}) + \hat{\varepsilon}_A(\boldsymbol{k}) + \hat{\varepsilon}_C(\boldsymbol{k}). \tag{3.16}$$

In equation (3.15) the rate-of-change term and the inertial term can usually be neglected because the moment of inertia is very small (as is done in our numerical scheme described below), giving

$$\hat{\Phi}^b(\boldsymbol{k}) + \hat{\Psi}_s(\boldsymbol{k}) - \hat{\varepsilon}_C(\boldsymbol{k}) = 0. \tag{3.17}$$

4. Fluid parameters

The governing equations contain a number of physical parameters which must be measured or estimated:

ν – kinematic viscosity
m – magnetic moment of a single particle
M_{sat} – saturation magnetization
τ – particle relaxation time
ζ – vortex viscosity
I – moment of inertia of a single particle
η' – spin viscosity
χ_o – initial magnetic susceptibility

The experimental fluid that we simulate is the water-based ferrofluid, EMG-206, from Ferrotec. The magnetite particles suspended in this fluid are assumed to have a mean magnetic diameter of $d_m = 10\,\text{nm}$. Ferrofluid particles are typically assumed to be 10 nm, because particles smaller than this lose their dipole moment, and particles larger exhibit significant particle-particle magnetic interaction. With the surfactant attached, the hydrodynamic diameter is approximately $d_h = 29.5\,\text{nm}$. These values are typical for ferrofluids. Due to a magnetically dead outer layer of magnetite on a particle, the actual diameter of the solid particle, d_s, is slightly larger than d_m. The particles in the system are assumed to be monodisperse and non-agglomerating due to the high shear rates characteristic of turbulent flows. The justification is based on experiments that suggest that agglomerations and chains of ferrofluid particles break apart in the presence of a strong shear (Odenbach 2002). The system is taken to be at a standard temperature of $T = 298.15\,\text{K}$.

Many of the fluid properties were determined by Schumacher *et al.* (2003): $\mu = 3.85 \times 10^{-3}\text{Pa s}$; $\rho = 1187.4\,\text{kg m}^{-3}$; thus, $\nu = \mu/\rho = 3.24 \times 10^{-6}\,\text{m}^2\,\text{s}^{-1}$. The magnetic moment of an individual particle is determined via $m = \pi d_m^3 M_{s,solid}/6$, where $M_{s,solid}$ is the saturation magnetization of the magnetite, $478\,\text{kA m}^{-1}$. Thus, $m = 2.5 \times 10^{-19}\,\text{A m}^2$.

The saturation magnetization of EMG-206 was obtained from data taken by Energy International, Bellevue, Washington. A value of $M_s = 164\,\text{Oe}$ is determined by plotting M vs. $1/H$ and extrapolating to $1/H = 0$ (see Schumacher 2005, Appendix B). The magnetic particle relaxation time refers to the time it takes for a ferrofluid particle to reorient its magnetization vector with an external field. Two types of relaxation times are relevant: Brownian and Néel. The Brownian relaxation time refers to when the magnetic moment is rigidly fixed within the particle and the particle has to rotate itself to align with an applied field. The Néel relaxation time refers to when the magnetization moment is free to rotate inside the particle without the particle having to move. For particles with diameters greater than 10 nm, Brownian relaxation is much faster than Néel relaxation; thus, the Néel component is ignored here and the relaxation time, τ, is equal to the Brownian relaxation time, τ_B. Shliomis (1972) relates the Brownian relaxation time to the effective hydrodynamic volume, V_h, which is the volume of the particle with the surfactant attached, and the dynamic viscosity of the carrier fluid, μ_c,

$$\tau_B = \frac{3V_h\mu_c}{k_BT}, \tag{4.1}$$

where k_BT is the thermal energy. Any agglomeration that occurs in real fluids leads to larger relaxation times. For this fluid, the relaxation time is estimated to be 10 μs.

The vortex viscosity, ζ, is the coefficient in the rate of transfer of internal to external angular momentum. In the energy equations, it appears as a proportionality constant of a rate of dissipation when the particles spin at a different rate than half the vorticity. Here, the vortex viscosity is estimated according to $\zeta = 1.5\mu\phi_h$ (Rosensweig

1985), where ϕ_h is the hydrodynamic volume fraction of the particles. Using this method for EMG-206, Schumacher *et al.* (2003) estimated $\zeta/\mu = 0.50$. Replacing the $M_{sat} = 11.94\,\mathrm{kA\,m^{-1}}$ used by Schumacher *et al.* (2003) with $M_{sat} = 13.05\,\mathrm{kA\,m^{-1}}$ gives $\zeta/\mu = 0.55$. Feng *et al.* (2006) provide a computational method for determining the vortex viscosity as a function of concentration.

If the ferrofluid particle is considered as a two-layered sphere with different densities in each layer, the moment of inertia per unit mass, I, is

$$I = \frac{\frac{8}{15}\pi\left[\rho_1 R_1^5 + \rho_2\left(R_2^5 - R_1^5\right)\right]}{\frac{4}{3}\pi\left[\left(\rho_1 - \rho_2\right)R_1^3 + \rho_2 R_2^3\right]}. \tag{4.2}$$

Thus, for a ferrofluid solution with particles of core density $\rho_1 = 5420\,\mathrm{kg\,m^{-3}}$, outer density $\rho_2 = 1000\,\mathrm{kg\,m^{-3}}$, core radius $R_1 = 5\times10^{-9}\,\mathrm{m}$, and overall radius $R_2 = 14.75\times10^{-9}\,\mathrm{m}$ the moment of inertia is $I = 7.57\times10^{-17}\,\mathrm{m^2}$.

The spin viscosity is the transport coefficient that relates the couple stress to the spin gradient. The spin viscosity has never been measured experimentally; however, Bou-Reslan (2002) uses Brownian Dynamics computer simulations to estimate a value of $\eta' = 2\times10^{-15}\,\mathrm{kg\,m\,s^{-1}}$.

The Felderhof & Kroh (1999) magnetization equation requires a value for the initial susceptibility of the ferrofluid. We use the relationship

$$\chi_o = \frac{\mu_o M_s m}{3k_B T}, \tag{4.3}$$

from Felderhof & Kroh (1999) to obtain a value of $\chi_o = 0.332$.

The moment of inertia of the ferrofluid particle is so small that the substantial derivative term in the spin equation can be ignored. The spin viscosity is also very small and the spin diffusion term can possibly be neglected; this is verified for the homogeneous simulations. The magnetic body force term in the momentum equation, $\mu_o M\cdot\nabla H$, and convection term in the magnetization equation, $\boldsymbol{u}\cdot\nabla\boldsymbol{M}$, are expected to be small, and we verify that they are negligible.

The moment of inertia of a ferrofluid particle is very small, and the estimate of the ferrofluid spin viscosity is also small. Therefore, it is often assumed that the terms in the spin equation that contain these parameters are negligible. An order of magnitude estimate shows the 'smallness' of these terms. The first term in the spin equation, $\rho I\partial\boldsymbol{\omega}/\partial t$, contains the moment of inertia. In the constituted form of the spin equation (2.4), the spin diffusion term, $\eta'\nabla^2\boldsymbol{\omega}$, contains the spin viscosity. Estimates of these two terms are compared to an estimate of the $-4\zeta\boldsymbol{\omega}$ term on the right-hand side to give the ratios

$$\frac{\rho I}{\tau\zeta}, \quad \frac{\eta'}{\ell^2\zeta}. \tag{4.4a, b}$$

We specify τ to be the particle relaxation time, τ_B, 10 µs, and specify ℓ to be the Taylor turbulence scale, λ, defined below; we obtain

$$\frac{\rho I}{\tau_B\zeta} \sim 5\times10^{-6}, \quad \frac{\eta'}{\lambda^2\zeta} \sim 7\times10^{-5}. \tag{4.5a, b}$$

Both of these ratios are much less than 1; the spin diffusion term may become important as the Kolmogorov scale becomes smaller, and the effect of the $\eta'\nabla^2\omega$ term is examined numerically in § 6.

5. Numerical analysis

5.1. *Numerical details*

Homogeneous turbulence is simulated in a cube of dimension L, where L is large relative to the integral scale of turbulence within the cube, $\mathscr{L}$. The cubic domain is discretized by choosing a sufficiently dense mesh such that the smallest scales of motion are resolved. The fluctuating dependent variables are treated as periodic functions and expanded in terms of a finite Fourier series in all three dimensions. The boundary conditions of all dependent variables exhibit periodicity in all three dimensions. For example, the velocity and pressure are represented as

$$\boldsymbol{u}(\boldsymbol{x}) = \sum_{k_x=-N/2}^{N/2} \sum_{k_y=-N/2}^{N/2} \sum_{k_z=-N/2}^{N/2} \hat{\boldsymbol{u}}(\boldsymbol{k})\, \mathrm{e}^{\mathrm{i}k\cdot x}, \tag{5.1a}$$

$$\pi(\boldsymbol{x}) = \frac{p(\boldsymbol{x})}{\rho} = \sum_{k_x=-N/2}^{N/2} \sum_{k_y=-N/2}^{N/2} \sum_{k_z=-N/2}^{N/2} \hat{\pi}(\boldsymbol{k})\, \mathrm{e}^{\mathrm{i}k\cdot x}, \tag{5.1b}$$

where k_x, k_y, and k_z are the wavenumbers ranging from $-N/2$ to $N/2$. Similar expansions are done for spin, magnetization, and the magnetic field. In physical space the dependent variables are real functions of space; therefore, the Fourier coefficients for these variables satisfy conjugate symmetry, e.g. $\hat{\boldsymbol{u}}(\boldsymbol{k}) = \hat{\boldsymbol{u}}^*(-\boldsymbol{k})$. Spectral methods are used; derivatives are computed in Fourier space and nonlinear terms are computed in physical space.

Recall that the complete set of ferrohydrodynamic governing equations contains five times as many nonlinear terms as the Navier–Stokes equations, and in order to compute each nonlinear term, the relevant variables and derivatives are inverse fast-Fourier transformed from wavenumber to physical space and then the nonlinear term is evaluated. The nonlinear terms are subsequently fast-Fourier transformed back to wavenumber space. In our code, the full ferrohydrodynamic simulation involves 45 total transformations per time step, whereas the Navier–Stokes simulations require only nine. Since approximately 90 % of the computational effort is spent in doing Fourier transformations, significantly greater computational resources are required relative to an analogous Newtonian case.

The average component of $\boldsymbol{H}$, i.e. $\hat{H}_{(0,0,0)}$, is a specified function of time that is related to the applied magnetic field, $\hat{H}_{0_x}$, by

$$\hat{H}_{x(0,0,0)} = \hat{H}_{o_x}, \quad \hat{H}_{y(0,0,0)} = 0, \quad \hat{H}_{z(0,0,0)} + \hat{M}_{z(0,0,0)} = \hat{B}_{o_z}/\mu_o = 0. \tag{5.2a–c}$$

These relationships are enforced by direct substitution into the (0,0,0) Fourier mode.

The code was subjected to two primary verification tests. First, the Taylor–Green vortex problem is solved analytically for short times and compared with results by Taylor & Green (1937). Second, the time-averaged torque is computed in a simplified system and compared to the results of the analytic solution of Zahn & Greer (1995). Details are available elsewhere (Schumacher 2005).

5.2. *Initial velocity*

Fully developed and steady-state turbulent ferrofluid flow through a 0.3 cm diameter tube at $Re \sim 3100$ has been studied experimentally and simulated numerically using a modified low-Reynolds-number k–ε model (Schumacher *et al.* 2003); in that case, the local flow near the centre of the tube had a translational turbulent kinetic energy of $E_t = 657\,\mathrm{cm^2\,s^{-2}}$. The root-mean-square (RMS) velocity is related to the translational

turbulent kinetic energy by

$$E_t = \frac{3}{2}u_{RMS}^2. \tag{5.3}$$

Therefore, $u_{RMS} \sim 20.9\,\mathrm{cm\,s^{-1}}$. According to McComb (1990), the Taylor-microscale Reynolds number, $Re_\lambda = \lambda u_{RMS}/\nu$, can be estimated using $Re_\lambda = 0.95Re^{7/16}$, which gives $Re_\lambda \sim 32$ for this case. Once the Taylor-microscale Reynolds number is estimated, the Taylor microscale can then be calculated,

$$\lambda = Re_\lambda \nu/u_{RMS} \approx 0.05\,\mathrm{cm}, \text{ where the Taylor microscale is } \lambda = \sqrt{(10\nu E_t)/\varepsilon}.$$

The length of one side of the cubic domain is taken as $L = 10\lambda = 0.48\,\mathrm{cm}$, which is five times the integral scale, $\mathscr{L}$.

The homogeneous ferrofluid flows that we report in this paper have flow properties that resemble this experimental case. Kerr (1985) performed DNS calculations of homogeneous flows with a range of $Re_\lambda = 28.5$–55.9 using 64^3 modes, and this number of modes was adequate for full resolution of the flow. Re_λ for our flow is relatively low; for comparison, Gotoh, Fukayama & Nakano (2002) did simulations at $Re_\lambda = 460$ using 1024^3 nodes and Kaneda *et al.* (2003) did simulations at $Re_\lambda = 1200$ with 4096^3 grid points. Because the flow we are interested in here occurs at a modest Re_λ, the full homogeneous simulations are feasible using the computational resources of a single desktop PC; we employ 64^3 modes in our simulations.

For the ferrofluid simulations, the flow is forced by injecting energy at low wavenumbers, and we allow the flow to develop in the absence of a magnetic field for six large-eddy turnover times. A single large-eddy turnover time is defined as

$$\mathscr{T} = \frac{\mathscr{L}}{u_{RMS}}, \tag{5.4}$$

where

$$\mathscr{L} = \frac{\pi}{2u_{RMS}^2}\int_{k=0}^{\infty}\frac{E_t(k)}{k}\mathrm{d}k \tag{5.5}$$

is the integral length scale. This gives ample time for the flow to 'relax' from its imposed initial conditions, and it allows the forced turbulence to reach a statistically stationary state by the time that the magnetic field is turned on. The magnetic field is turned on at the beginning of the sixth large-eddy turnover time. In order to obtain a statistically stationary state, energy is injected into the flow at the largest scales. Forced simulations compensate for the energy dissipated at small scales by injecting energy into the large scales. Further, the use of forcing helps to alleviate some of the complications with interpreting the time-evolving turbulence scales of decaying turbulence (Sundaram & Collins 1997). For the simulations here, energy injection is performed after each velocity update. All wavenumber modes less than $2.5k_{min}$ are considered to be within a forcing shell, and the energy within the forcing shell is kept constant throughout the entire simulation in the following manner. After the velocity is advanced one time step, the Fourier modes within the forcing shell are all multiplied by the value necessary for the energy in the forcing shell to be the same as it was prior to the time step. This forcing scheme, used by Zikanov & Thess (1998), helps minimize the artificial effects of energy injection.

To simulate the flow case with the magnetic field applied, the energy in the forcing shell is set to equal 70 % of the turbulent kinetic energy at the centre of the pipe. The flow was allowed to develop for 12 large-eddy turnover times, and the flow statistics reported in table 2 represent flow properties that are time-averaged over the

u_{RMS}	$20.63\,\mathrm{cm\,s^{-1}}$	$\mathscr{L}$	0.1 cm
ε	$60\,400\,\mathrm{cm^2\ s^{-3}}$	$\mathscr{T}$	0.00485 s
λ	0.0586 cm	η	0.00487 cm
Re_λ	37.3	τ_η	7.324×10^{-4} s
$k_{\max}\eta$	2.0	Δt	1.5×10^{-5} s

TABLE 2. Time averages over the final six large-eddy turnover times of the homogeneous simulation.

final six large-eddy turnover times. Notice in table 2 that the properties $Re_\lambda = 37.3$, $E_t \sim 648\,\mathrm{cm^2\,s^{-2}}$ (where E_t is computed using u_{RMS}), and $\lambda = 0.0586\,\mathrm{cm}$ are all close to the properties estimated at the centre of the pipe. When $k_{\max}\eta \geqslant 1.5$, the smallest scales of motion are well resolved (Pope 2000). From table 2, $k_{\max}\eta \sim 2.0$ exceeds this requirement; thus, the small scales of the turbulent flow are adequately resolved. The initial velocity field for the ferrofluid simulations is representative of the homogeneous turbulence at the centreline of the experimental flow, is in a statistically stationary state, and the smallest scales of the flow are well resolved.

5.3. *Length and time scales*

Turbulence naturally contains a wide range of length and time scales that must be resolved when doing accurate direct numerical simulations. The largest length scales determine the domain size and the smallest determine the density of mesh necessary to resolve all relevant motion. The time step required for accuracy and stability in a ferrofluid system can be very different from those for a Newtonian fluid. The primary characteristic times in the ferrofluid system in which we are interested are the Kolmogorov time of the turbulent flow, τ_η, and the relaxation time of the magnetic particles, τ_B; if the magnetic field were oscillating, the period of oscillation of the magnetic field, $2\pi/\Omega$, would become important. The time step required for an accurate solution depends upon each of these. Note that in the results reported here, the applied magnetic field $\hat{H}_{0_x}$ is held fixed in time.

For an accurate simulation of a Newtonian fluid, a fluid particle must not move more than a portion of the node spacing Δx (Pope 2000). Pope recommends using the Courant condition $(k^{0.5}\Delta t)/\Delta x = 1/20$ as a basis for choosing a time step size. The magnetization relaxation time that appears in the material magnetization equation is very small, $\sim 10\,\mu\mathrm{s}$. In many cases this causes the stable time step required for the solution of the magnetization equations to be much smaller than the Δt needed for an accurate solution of the momentum equations.

When there is a large separation of time scales due to a very small τ_B, one option is to use brute force and update the entire system of equations using a small enough Δt to ensure both the stability of the magnetization equation and accuracy of the momentum equation. However, if the velocity field changes slowly compared to the characteristic relaxation time, then it is reasonable to partially decouple the momentum and magnetization equations such that the magnetization equation is updated with very small time steps using a constant velocity field. After a certain number of time steps, the velocity field is updated. This subcycling method is used to significantly decrease the computational effort required to update the full set of governing equations for some simulations.

	Ferrofluid	Newtonian
E_t (cm^2 s^{-2})	634.51	634.51
T (cm^2 s^{-3})	0	0
ε (cm^2 s^{-3})	58418.6	58419.2
ε_A (cm^2 s^{-3})	3.9×10^{-5}	0
ε_C (cm^2 s^{-3})	0.61	0
Φ^b (cm^2 s^{-3})	0.61	0
λ (cm)	0.0594	0.0594
η (cm)	0.00491	0.00491
τ_η (s)	7.45×10^{-4}	7.45×10^{-4}
Re_λ	37.65	37.65

TABLE 3. Flow properties of a ferrofluid without a magnetic field and an analogous Newtonian fluid.

6. Results

6.1. *Magnetic field turned off*

The equations of motion for a ferrofluid flow with no applied magnetic field (and ignoring the terms involving moment of inertia) are

$$\rho\left(\frac{\partial \boldsymbol{u}}{\partial t} + \boldsymbol{u}\cdot\nabla\boldsymbol{u}\right) = -\nabla p + 2\mu\nabla\cdot\boldsymbol{e} + \zeta\nabla\times(2\boldsymbol{\omega} - \nabla\times\boldsymbol{u}), \tag{6.1}$$

$$0 = 2\eta'\nabla\cdot\boldsymbol{s} + 2\zeta(\nabla\times\boldsymbol{u} - 2\boldsymbol{\omega}), \tag{6.2}$$

$$\nabla\cdot\boldsymbol{u} = 0. \tag{6.3}$$

If the couple stress term $2\eta' s$ is negligible, then $2\zeta(\nabla\times\boldsymbol{u} - 2\boldsymbol{\omega}) = 0$, and the governing equations become the same as Navier–Stokes equations. The couple stress term is generally negligible for most ferrofluid flows because the spin viscosity and spin gradients are usually small. If turbulent motions or the presence of a solid boundary induce large spin gradients, this can lead to a couple stress that is no longer negligible, and the resulting spin and vortex viscous terms will induce non-Newtonian behaviour.

We compute the turbulent ferrofluid flow without a magnetic field, and we compare the results to a Newtonian simulation using the same parameters. Time-averaged results are summarized here in table 3. In the ferrofluid case the vortex rate of dissipation term, ε_A, and rotational kinetic energy rate of dissipation term, ε_C, are not exactly zero, but they are very small relative to the classical rate of viscous dissipation. Thus, these terms are essentially unimportant in this particular case. The difference between the ferrofluid case and the Newtonian case is so small that the ferrofluid system without a magnetic field can be accurately approximated as a Newtonian fluid.

The couple stress term starts to become important when $C_{\eta'} > 1$ (Schumacher 2005), where $C_{\eta'} = \eta'/(\eta^2\mu)$ is a non-dimensional coefficient in the normalized spin equation. This normalized equation can be obtained from the spin equation by using the velocity scale U and the Kolmogorov length scale η to non-dimensionalize it. In particular, spin is then non-dimensionalized with U/η, and the spin-rate gradient $\boldsymbol{s}$ with U/η^2. The result is the following, where the primes denote the non-dimensional quantity:

$$0 = 2\frac{\eta'}{\eta^2\mu}\nabla'\cdot\boldsymbol{s}' + 2\frac{\zeta}{\mu}(\nabla'\times\boldsymbol{u}' - 2\boldsymbol{\omega}'). \tag{6.4}$$

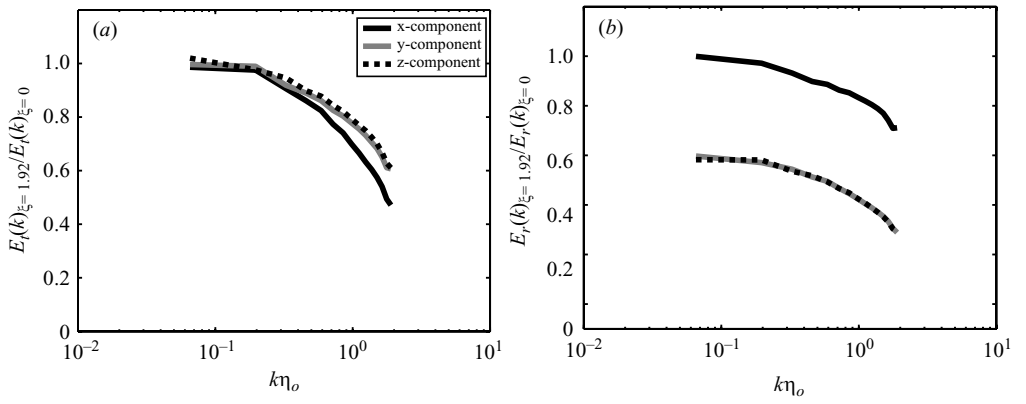

FIGURE 2. Spectra for $H_0 = 316$ Oe using the magnetization equation from Martsenyuk *et al.* (1974): (*a*) individual velocity components, (*b*) individual spin components. Both spectra are normalized using equations (34) and (35), respectively.

Thus, as the spin viscosity becomes larger and/or the Kolmogorov scale becomes smaller, spin effects grow in magnitude. For the ferrofluid here, $C_{\eta'} = 0.00025$. Thus, Newtonian fluid behaviour is expected.

6.2. *Steady magnetic field results*

In this section, we study the effect of applying a steady spatially uniform magnetic field to homogeneous turbulent ferrofluid flow (see equations (5.2*a–c*)). Although the applied field is spatially uniform, the turbulent flow of the magnetic liquid may induce magnetic field fluctuations. The full set of governing equations is solved using DNS. The effect of the magnetic field magnitude and the choice of magnetization equation are also examined. Three different magnitudes of magnetic field are considered here: 158 Oe ($\xi = 0.96$), 316 Oe ($\xi = 1.92$), and 1264 Oe ($\xi = 7.68$), where the values in parentheses represent the normalized magnitude defined by (2.23*b*). The three different material magnetization equations discussed previously (Shliomis 1972, (2.21); Martsenyuk *et al.* 1974, (2.26); and Felderhof & Kroh 2000, (2.24)) are also considered at each magnetic field strength. The results are compared to the case without a magnetic field, which is essentially the same as a Newtonian flow. For the cases reported here, the flow is solved in time over a span of four large-eddy turnover times.

For the first case discussed here, the complete set of ferrohydrodynamic equations is solved in conjunction with the magnetization equation proposed by Martsenyuk *et al.* (1974) with an applied field magnitude of 316 Oe ($\xi = 1.92$). First, we present results showing how the magnetic field affects the spectra of the kinetic energy of the components of the velocity field, figure 2. The time-averaged RMS velocity components for this magnetic field case are $u_x = 19.50\,\mathrm{cm\,s^{-1}}$, $u_y = 22.09\,\mathrm{cm\,s^{-1}}$, and $u_z = 19.39\,\mathrm{cm\,s^{-1}}$, and the same components in the magnetic-field-off case are $u_x = 19.84\,\mathrm{cm\,s^{-1}}$, $u_y = 22.16\,\mathrm{cm\,s^{-1}}$, and $u_z = 19.61\,\mathrm{cm\,s^{-1}}$. The magnetic field causes a very slight damping of the velocity fluctuations. Figure 2(*a*) shows how the spectra of the velocity components are affected at different wavenumbers. Specifically, the ratio

$$\frac{E_t}{E_{t0}} = \frac{\langle \hat{u}_{i,\xi=1.92}(k)\,\hat{u}^*_{i,\xi=1.92}(k)\rangle}{\langle \hat{u}_{i,\xi=0}(k)\,\hat{u}^*_{i,\xi=0}(k)\rangle} \tag{6.5}$$

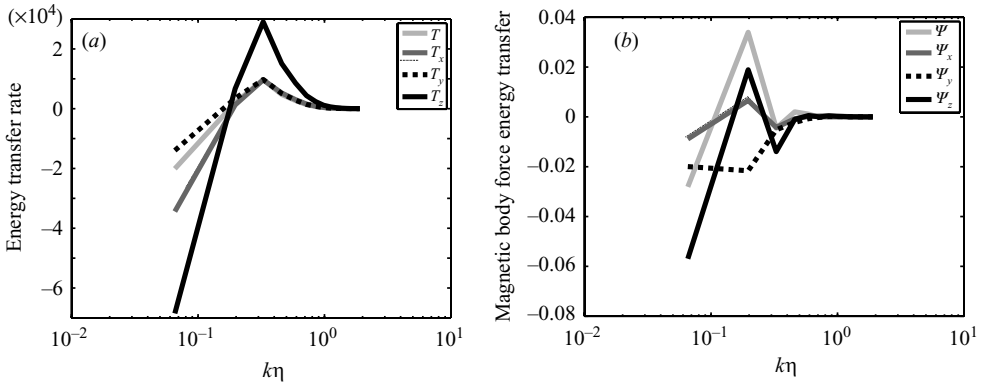

FIGURE 3. Spectra for $H_0 = 316$ Oe using the magnetization equation from Martsenyuk *et al.* (1974): (*a*) energy transfer rate, T; (*b*) energy transfer spectra due to the magnetic body force, Ψ.

is plotted vs. k, where the numerator represents the energy spectrum of the translational component in the magnetic field case and the denominator represents the corresponding component with the magnetic field turned off. Note that the averaged spectral quantities are computed by summing the Fourier amplitudes in shells in wavenumber space. Because the ratio is less than unity at all points outside the forcing range, the magnetic field decreases the spectral energy at all wavenumbers outside the forcing shell. At low wavenumbers the ratio is near 1 because of forcing. The slope for each component is negative, showing that the spectral energies are decreased more at smaller scales. Further, the velocity components that are perpendicular to the field (y- and z-directions) show a smaller damping effect compared to the velocity component that is parallel to the magnetic field (x-direction).

The time-averaged RMS spin components for the magnetic field case are $\omega_x = 369\,\mathrm{s}^{-1}$, $\omega_y = 310\,\mathrm{s}^{-1}$, $\omega_z = 295\,\mathrm{s}^{-1}$, and the same components with the magnetic field turned off are $\omega_x = 379\,\mathrm{s}^{-1}$, $\omega_y = 401\,\mathrm{s}^{-1}$, and $\omega_z = 381\,\mathrm{s}^{-1}$. Thus, the spin components perpendicular to the field (y- and z-directions) are severely damped relative to the magnetic-field-off case, while the spin component parallel to the magnetic field (x-direction) is slightly less than the magnetic-field-off case. These results show that the magnetic field has a strongly anisotropic effect on the fluctuating spin components. This is further illustrated in figure 2(*b*), which shows how the magnetic field influences the spin components over the wavenumber range. Specifically, the ratio

$$\frac{E_r}{E_{r0}} = \frac{\langle \hat{\omega}_{i,\,\xi=1.92}(k)\,\hat{\omega}^*_{i,\,\xi=1.92}(k)\rangle}{\langle \hat{\omega}_{i,\xi=0}(k)\,\hat{\omega}^*_{i,\xi=0}(k)\rangle} \tag{6.6}$$

is plotted versus k, where the numerator represents the energy spectrum of the rotational component in the magnetic field case and the denominator represents the component of the corresponding spectrum with the magnetic field turned off. The perpendicular rotational components (y- and z-directions) are severely damped at all wavenumbers, with the largest decrease occurring at large wavenumbers. The parallel rotational component (x-direction) is unchanged at low wavenumbers, but decreases at higher wavenumbers.

Next, consider the wavenumber distributions of the classical energy transfer rate, $\hat{T}(k)$, shown in figure 3(*a*), and the rate of energy conversion between kinetic and

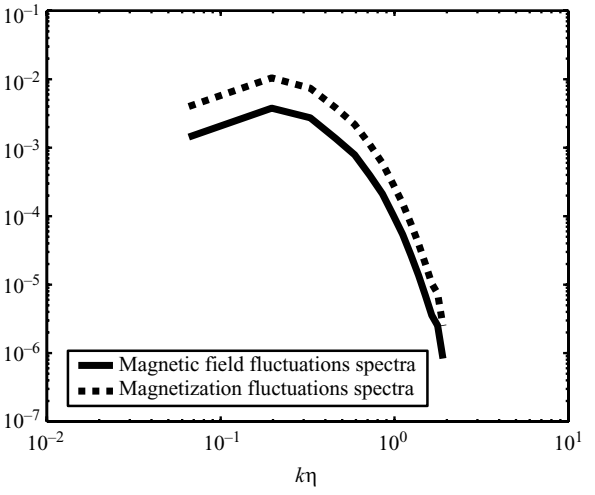

FIGURE 4. Spectra of the magnetic field fluctuations and the magnetization fluctuations.

magnetic modes, $\hat{\Psi}(k)$, shown in figure 3(*b*). The directional components of $\hat{T}_i(k)$ and $\hat{\Psi}_i(k)$ are also included in the panels of figure 3. The wavenumber distribution of $\hat{T}(k)$ shows an approximate minimum of $-7\times10^4\,\mathrm{cm^2\,s^{-3}}$ at the largest scale ($k\eta\sim0.06$) and an approximate maximum of $3\times10^4\,\mathrm{cm^2\,s^{-3}}$ at $k\eta=0.3$. The maximum and minimum values of $\hat{\Psi}(k)$, as seen in figure 3(*b*), are about six orders of magnitude smaller than those of $\hat{T}(k)$. The spatial averages of both these terms, further averaged over the four large-eddy times, give very small values of $\langle T\rangle$ and $\langle\Psi\rangle$, especially relative to other energy terms, for example $\langle\varepsilon\rangle\sim54000\,\mathrm{cm^2\,s^{-3}}$. The volume average $\langle T\rangle$ is approximately zero, within numerical round-off error, because the transfer rate term is conservative. The Ψ term is not conservative; however, the value of $\langle\Psi\rangle$ is still very small because the magnitude of $\hat{\Psi}(k)$ is so small over the entire range of wavenumbers. Thus, the magnetic body force term does not appear to play a significant role in this case. The other energy terms are studied below, and they depend on the magnitude of the magnetic field.

Next, we study the role that the fluctuating magnetic field and fluctuating magnetization have on the homogeneous flow. The root-mean-square magnetic field components are $H_x=0.049\,\mathrm{A\,cm^{-1}}$, $H_y=0.062\,\mathrm{A\,cm^{-1}}$, and $H_z=0.069\,\mathrm{A\,cm^{-1}}$, and the RMS magnetization components are $M_x=0.009\,\mathrm{A\,cm^{-1}}$, $M_y=0.120\,\mathrm{A\,cm^{-1}}$, and $M_z=0.125\,\mathrm{A\,cm^{-1}}$; these components are all zero in the magnetic-field-off case. For comparison, the applied magnetic field is $\overline{\boldsymbol{H}}=251\,\mathrm{A\,cm^{-1}}$ (316 Oe) and the mean induced magnetization due to the applied field is $\overline{\boldsymbol{M}}=68.3\,\mathrm{A\,cm^{-1}}$. Figure 4 shows the magnetic field fluctuation spectra and the magnetization fluctuation spectra. The fluctuations that occur in this flow are very small relative to the applied field and induced magnetization. Since the flow is sensitive to $\boldsymbol{H}$ and $\boldsymbol{M}$, and since $\mathrm{H_{RMS}}$ and $\mathrm{M_{RMS}}$ are much smaller in magnitude relative to $\overline{\boldsymbol{H}}$ and $\overline{\boldsymbol{M}}$, respectively, then the fluctuating magnetic components will probably have a negligible influence on the flow. We validated this by performing another simulation, under the same conditions, that neglects the magnetic body force in the momentum equation and magnetic convection terms in the magnetization equation. The flow results are the same as the simulations that use the full set of equations. Thus, the magnetic body force and magnetic convection terms can be ignored, and they are neglected in the

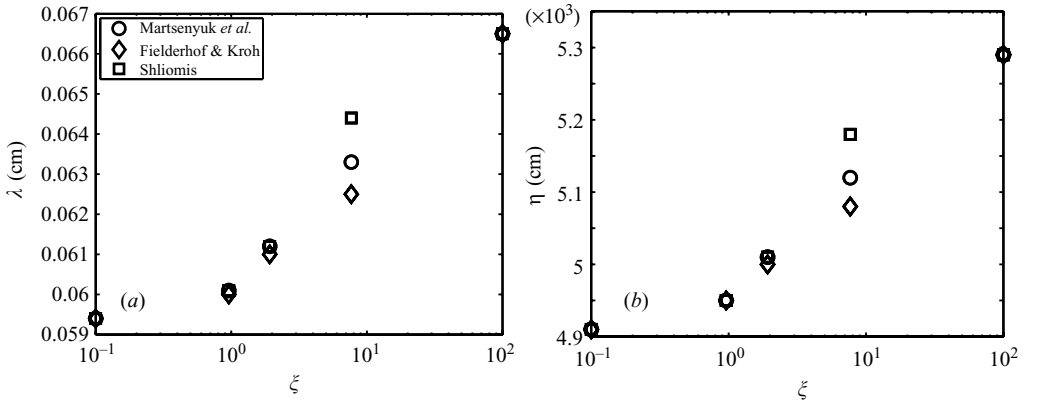

FIGURE 5. Effect of magnetic field on the averaged turbulence length scales; (*a*) Taylor microscale; (*b*) Kolmogorov turbulence scale. The data point at $\xi = 0.1$ represents the case with no magnetic field; the data point at $\xi = 100$ represents an infinite magnetic field.

remaining simulations here. Without those two terms the total number of Fourier transformations is reduced from 45 to 27, which provides significant computational savings; even so the simulations are still much more intensive than a Newtonian case.

6.3. *Effect of magnetic field magnitude*

The effect on the turbulent system by increasing the magnetic field magnitude is studied next. Take a steady uniform applied magnetic field in the x-direction only. The non-dimensional magnitudes of the fields considered are $\xi = 0, 0.96, 1.92, 7.68$, and infinity. The infinite magnetic field is approximated by artificially setting the spin components transverse to the field to zero at all times in the simulation. For each applied magnetic field magnitude, a separate flow is solved for each of the three different magnetization equations considered in this paper. The effects of the three different magnetization equations are discussed in § 6.4.

As shown in figure 5, the time-averaged length scales become larger with magnetic field strength and shift upwards towards the $\xi =$ infinity case as ξ becomes larger. In going from $\xi = 0$ to 7.68, the Taylor microscale and Kolmogorov microscale increase by about 7 % and 5 %, respectively, and in going from $\xi = 0$ to ∞, they increase by about 12 % and 8 %, respectively. The effects of the magnetic field strength on the RMS values of velocity and spin are shown in figure 6. Here, the RMS velocity and spin become smaller with magnetic field and shift downwards toward the infinity case as ξ becomes larger. When going from $\xi = 0$ to 7.68, the RMS velocity and spin decrease by about 1.8 % and 39 %, respectively, and in going from $\xi = 0$ to ∞, they decrease by about 3.3 % and 71 %, respectively.

Without an applied field, the simulated turbulent velocity, vorticity, and spin fields are approximately isotropic. The root-mean-square components of the spin are presented in table 4 as a function of the magnetic field parameter, ξ. Notice that the RMS components of spin transverse to the applied field become much smaller than the component parallel to the field, so that the spin field exhibits a highly anisotropic behaviour in the presence of an applied field.

Since the magnetic body force is neglected, the sink/source term due to this term, $\hat{\Psi}(k)$, is zero. The left-hand side of the rotational energy equation is also neglected. This means that energy transferred to the rotational modes is not accumulated but,

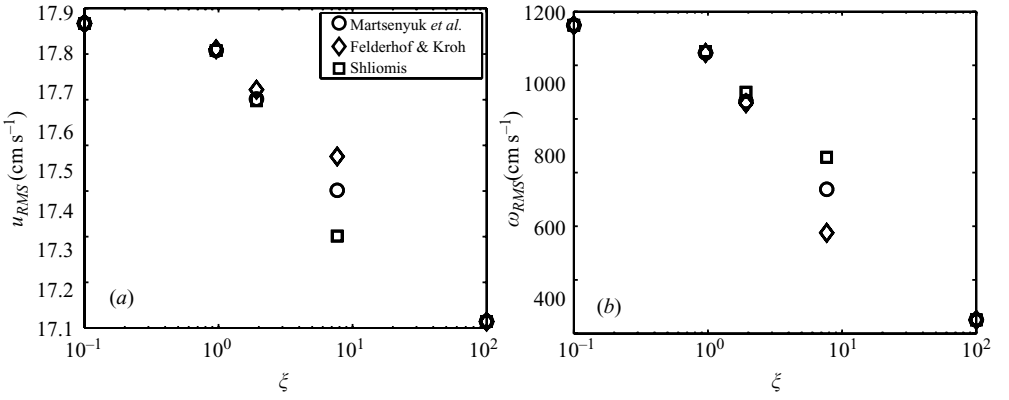

FIGURE 6. Effect of magnetic field on the RMS values when using different magnization equations; (*a*) velocity, and (*b*) spin. The data point at $\xi = 0.1$ represents the magnetic field off case. The data point at $\xi = 100$ represents an infinite magnetic field.

ξ:	0	0.96	1.92	7.68	∞
$2\omega_x$ (s^{-1})	758	750	736	710	677
$2\omega_y$ (s^{-1})	803	728	591	357	0
$2\omega_z$ (s^{-1})	762	691	561	339	0

TABLE 4. Effect of magnetic field on time-averaged spin vector.

rather, instantly redistributed to kinetic, internal, and magnetic energies such that $\hat{\Phi}^b(k) + \hat{\Psi}_s(k) - \hat{\varepsilon}_C(k)$ is zero. The energy equations, (3.14)–(3.16), summed over all wavenumbers, are

$$\frac{\mathrm{d}E_t}{\mathrm{d}t} = T - \varepsilon_A - \Phi^b - \varepsilon, \tag{6.7}$$

$$\Phi^b + \Psi_s - \varepsilon_C = 0, \tag{6.8}$$

$$\frac{\mathrm{d}U}{\mathrm{d}t} = \varepsilon + \varepsilon_A + \varepsilon_C. \tag{6.9}$$

In order to study how the magnetic field magnitude influences the energetics, the time-average of each term, except the internal energy, U, is tracked as the magnetic field increases. The time-averaged values of ε, ε_A, ε_C, Φ^b, and Ψ_s are presented in figure 7. The values of the classical viscous dissipation rate, ε, decrease as the magnetic field is increased. The vortex viscous dissipation rate, ε_A, increases with ξ. The rotational kinetic energy dissipation rate, ε_C, decreases with ξ. The transfer of energy from kinetic to rotational modes, Φ^b, increases with ξ up to $\xi = 7.68$. However, on going from $\xi = 7.68$ to ∞, Φ^b decreases. The rate of loss of E in a Newtonian fluid is ε, and in a ferrofluid is the sum $\varepsilon + \varepsilon_A + \Phi^b$, and this is approximately constant (not shown). Thus, the rate of loss of kinetic energy in each case can be reasonably approximated using the total ε in the Newtonian fluid case.

6.4. *Effect of magnetization equation*

Next consider the effect of the magnetization equation at different magnetic field magnitudes and for all three magnetization equations. Figures 5 and 6 show that the choice of magnetization equation can affect the characteristics (e.g. λ, η, u_{RMS}, and

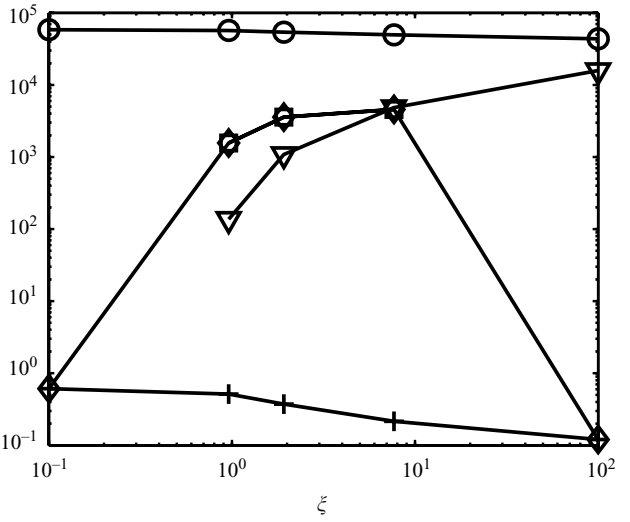

FIGURE 7. Effect of magnetic field magnitude on averaged energy terms: ○, ε (cm^2 s^{-3}); ∇, ε_A (cm^2 s^{-3}); □, ψ_s (cm^2 s^{-3}); ◇, ϕ^B (cm^2 s^{-3}); $+\varepsilon_C$ (cm^2 s^{-3}). The data point at $\xi = 0.1$ represents the magnetic-field-off case. The data point at $\xi = 100$ represents an infinite magnetic field. The Shliomis (1972) magnetization is used when $\xi \leqslant 2$, and the Martsenyuk *et al.* (1974) magnetization equation is used when $\xi > 2$. The square symbols (representing Ψ_s) and the diamond symbols (representing ϕ^b) are essentially superimposed. Since $\phi^b + \Psi_s - \varepsilon_c = 0$, and ε_c is very small, $\phi^b \approx -\Psi_s$.

ω_{RMS}) of computed turbulent flow at large magnetic field magnitudes. For example, at $\xi = 7.68$, the λ, η, u_{RMS}, and ω_{RMS} predicted by (2.21) and (2.26) differ by 1.7 %, 1.2 %, 0.5 %, and 21 %, respectively.

According to the governing equations, the magnetic field affects the flow through the magnetic body force and magnetic body couple terms. Because the magnetic body force is negligible in the cases we are studying, the magnetic field affects the flow via the torque in the spin equation since this is the only term remaining in the hydrodynamic equations that contains magnetization. To further understand how the various magnetization equations affect the mechanics of the flow, we focus on how the chosen magnetization equation affects the temporal development of the spatially averaged body torque. Figure 8 shows the development in time of the root-mean-square torque, $\mu_o/2\zeta\langle \boldsymbol{M} \times \boldsymbol{H} \rangle$, where figure 8(*b*) focuses on the fast initial transition region after the magnetic field is turned on. When the magnetic field is small ($\xi = 0.24$ and 0.96), the torque does not significantly depend on the choice of magnetization equation, and the turbulence results are essentially the same (as shown in figures 5 and 6). However, at larger magnetic fields ($\xi = 7.68$), the torque term is significantly affected by the choice of the particular magnetization equation which leads to turbulent flows with different characteristics. From figure 8(*b*), the differences in the torque are apparent after a very short time proportional to the magnetic relaxation time. The torque affects the difference between particle spin and fluid vorticity (2.11). Since the constitutive equation for the asymmetric stress is proportional to the difference of spin and vorticity (see § 2.1), it is no surprise that when the magnetic field is large the differences in body torques, due to the different magnetization equations, have an impact on the resulting turbulent flow as illustrated in figures 5 and 6.

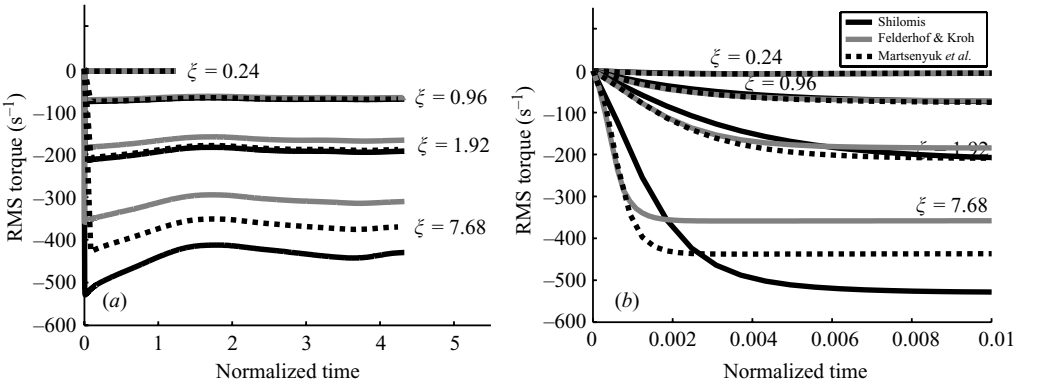

FIGURE 8. Root-mean-square of the body torque, $\mu_o/2\zeta\langle M \times H\rangle$, versus time normalized by the large-eddy turnover time; (*a*) over the entire simulation time; (*b*) with a focus on the short time scales.

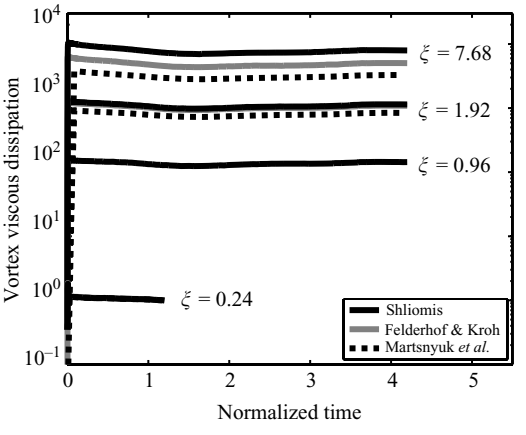

FIGURE 9. Vortex viscous dissipation rate, ε_A versus time normalized by the large-eddy turnover time.

The vortex rate of viscous dissipation is proportional to the square of the difference between spin and half the vorticity, and thus it is very sensitive to magnetic field amplitude and the choice of magnetization equation. Figure 9 shows the vortex rate of viscous dissipation versus time for four different magnitudes of magnetic field strength and for all three magnetization equations. At the lowest magnetic field magnitude, $\xi = 0.24$, the results are superimposed and thus independent of the magnetization equation used. At medium field strengths ($\xi = 0.96$ and 1.92) the vortex rate of viscous dissipation shows a dependence on magnetization equation, but the differences are not large. At high magnetic field strengths ($\xi = 7.68$) the differences in results are large. This result is consistent with the laminar results of Felderhof (2001), who studied the effects of the three different magnetization equations on ferrofluid pipe flow with an applied axial magnetic field. Felderhof's results show that for low magnitudes of the magnetic field, $\xi < 2$, the theoretically predicted magnetoviscosity is essentially independent of the choice of magnetization equation.

There are also a number of other parameters that have a small effect (Schumacher 2005). For vortex viscosities 10 %, 55 %, and 100 % of the shear viscosity, the turbulent

kinetic energy and rate of viscous dissipation terms vary by no more than 10 %; the vortex rate of viscous dissipation varies greatly, as expected, but it is still a small part of the total rate of dissipation. The effect of the saturation magnetization (from 0 to 260) is to increase the Taylor and Kolmogorov microscale lengths by only 3–5 %. The saturation magnetization does affect the kinetic energy spectrum and especially the rotational kinetic energy, and these effects are large at large wavenumbers. The ratio of the Brownian time constant to the Komolgorov turbulent time constant was investigated for ratios of 0.002, 0.01, 0.5, and 1. For the smallest ratio, the Taylor and Kolmogorov microscale lengths increased by 3 % and 2 %, respectively. For a ratio of 1.0, the increases are 8 % and 12 %, respectively. The total kinetic energy decreases by 10 % when the ratio is increased by a factor of 100.

7. Conclusions

The general equations necessary for a basic theoretical interpretation of the physics of turbulence in ferrofluids are derived. The equations show multiple novel turbulence aspects that arise in ferrofluids. For example, two new modes of turbulent kinetic energy dissipation rate occur and unique modes of energy conversion (rotational to/from translational kinetic energy and magnetic energy to/from turbulent kinetic energy) are exhibited in turbulent ferrofluid flows. Furthermore, it is shown that potential modes for turbulence in ferrofluids are complicated by additional closure requirements from the five new nonlinear terms in the governing equations.

For turbulence of a ferrofluid in the presence of a steady magnetic field (as well as the case of no magnetic field) certain terms in the equations are shown to be unimportant. A ferrofluid with an applied magnetic field gives enhanced anisotropy of the turbulence, and the turbulence properties (both old ones and new ones) vary with the strength of the magnetic field. While a ferrofluid has new modes of viscous dissipation, the total rate of viscous dissipation is almost the same as for a Newtonian fluid with the same physical properties. The magnetization equations of Shliomis (1972), Martsenyuk *et al.* (1974), and Felderhof & Kroh (1999) give similar turbulence results at smaller magnetic fields ($\xi < 2$). Thus, the simplest magnetization equation (2.21), which requires fewer computations and is more easily implemented than either (2.24) or (2.26), can be used effectively in turbulent flows at low magnetic fields, namely $\xi < 2$. However, for larger magnetic fields the three different magnetization equations give different turbulent flow results.

This work was supported in part by NSF Grant CTS–347044.

REFERENCES

Anton, A. 1990 Measurements of turbulence suppression due to a transverse magnetic field applied on a ferrofluid motion. *J. Magn. Magn. Mater.* **85**, 137–140.

Bacri, J., Perzynski, R., Shliomis, M. & Burde, G. 1995 "Negative-viscosity" effect in a magnetic fluid. *Phys. Rev. Lett.* **75**, 2128–2131.

Berger, M., Castelino, J., Huang, R., Shah, M. & Austin, R. 2001 Design of a microfabricated magnetic cell separator. *Electrophoresis* **22**, 3883.

Bou-Reslan, D. 2002 Brownian dynamics simulation of ferromagnetic fluid in the vicinity of a solid wall in simple shear flow. Masters Thesis, University of Illinois at Chicago.

Brenner, H. & Nadim, A. 1996 The Lorentz reciprocal theorem for micropolar fluids. *J. Engng Maths* **30**, 169–176.

Dahler, J. & Scriven, L. 1961 Angular momentum of continua. *Nature* **192**, 36–37.

Dahler, J. & Scriven, L. 1963 Theory of structured continua. I. General consideration of angular momentum and polarization. *Proc. R. Soc. Lond.* A **275**, 504–527.

Felderhof, B. 2001 Flow of a ferrofluid down a tube in an oscillating magnetic field. *Phys. Rev.* E **64**, 21508.

Felderhof, B. & Kroh, H. 1999 Hydrodynamics of magnetic and dielectric fluids in interaction with the electromagnetic field. *J. Chem. Phys.* **110**, 7403.

Feng, S., Graham, A., Abbott, J. & Brenner, H. 2006 Antisymmetric stresses in suspensions: Vortex viscosity and energy dissipation. *J. Fluid Mech.* **563**, 97–122.

Gotoh, T., Fukayama, D. & Nakano, T. 2002 Velocity field statistics in homogeneous steady turbulence obtained using a high-resolution direct numerical simulation. *Phys. Fluids* **14**, 1065.

Kamiyama, S. 1996 Pipe flow problems. In *Magnetic Fluids and Applications Handbook* (ed. B. Berkovski), pp. 471–503. Begell House.

Kaneda, Y., Ishihara, T., Yokokawa, M., Itakura, K. & Uno, A. 2003 Energy dissipation rate and energy spectrum in high resolution direct numerical simulations of turbulence in a periodic box. *Phys. Fluids* **15**, L21–L24.

Kerr, R. 1985 Higher-order derivative correlations and the alignment of small-scale structures in isotropic numerical turbulence. *J. Fluid Mech.* **153**, 31–58.

Krekhov, A., Shliomis, M. & Kamiyama, S. 2005 Ferrofluid pipe flow in an oscillating magnetic field. *Phys. Fluids* **17**, 033105.

Lubbe, A., Alexiou, C. & Bergemann, C. 2001 Clinical applications of magnetic drug targeting. *J. Surg. Res.* **95**, 200–206.

Martsenyuk, M., Raikher, Y. & Shliomis, M. 1974 On the kinetics of magnetization of suspensions of ferromagnetic particles. *Sov. Phys. JETP* **38**, 413.

McComb, W. D. 1990 *The Physics of Fluid Turbulence*. Oxford University Press, Oxford.

McTague, J. 1969 Magnetoviscosity of magnetic colloids. *J. Chem. Phys.* **51**, 133.

Moskowitz, R. & Rosensweig, R. 1967 Nonmechanical torque driven flow in magnetic suspensions. *Appl. Phys. Lett.* **11**, 1967.

Odenbach, S. 2002 *Magnetoviscous effects in ferrofluids*. Lecture Notes in Physics, Monographs **71**, Springer.

Pope, S. B. 2000 *Turbulent Flows*. Cambridge University Press.

Ramchand, C., Priyadarshini, P., Kopcansky, P. & Mehta, R. 2001 Application of magnetic fluids in medicine and biotechnology. *Indian J. Pure Appl. Phys.* **39**, 683–686.

Roger, J., Pons, J., Massart, R., Halbreich, A. & Bacri, J. 1999 Some biomedical applications of ferrofluids. *Eur. Phys. J.* As **5**, 321–325.

Rosensweig, R. E. 1985 *Ferrohydrodynamics*. Cambridge University Press; reprinted by Dover, Mineola, NY, 1997.

Schumacher, K. R. 2005 Direct numerical simulation of ferrofluid turbulence in magnetic fields. PhD Thesis, University of Washington.

Schumacher, K., Sellien, I., Knoke, G., Cader, T. & Finlayson, B. 2003 Experiment and simulation of laminar and turbulent ferrofluid pipe flow in an oscillating magnetic field. *Phys. Rev.* E **67**, 26308.

Shliomis, M. 1972 Effective viscosity of magnetic suspensions. *Sov. Phys. JETP* **34**, 1291–1294.

Shliomis, M. & Morozov, K. 1994 Negative viscosity of ferrofluid under alternating magnetic field. *Phys. Fluids* **6**, 2855.

Snyder, S., Cader, T. & Finlayson, B. 2003 Finite element model of magnetoconvection of a ferrofluid. *J. Magn. Magn. Mater.* **262**, 269–279.

Sundaram, S. & Collins, L. 1997 Collision statistics in an isotropic particle-laden turbulent suspension. Part 1. Direct numerical simulations. *J. Fluid Mech.* **335**, 75–109.

Taylor, G. & Green, A. 1937 Mechanism of the production of small eddies from large ones. *Proc. R. Soc. Lond.* A **158**, 499–521.

Zahn, M. & Greer, D. 1995 Ferrohydrodynamic pumping in spatially uniform sinusoidally time-varying magnetic fields. *J. Magn. Magn. Mater.* **149**, 165–173.

Zeuner, A., Richter, R. & Rehberg, I. 1998 Experiments on negative and positive magnetoviscosity in an alternating magnetic field. *Phys. Rev.* E **58**, 6287–6293.

Zikanov, O. & Thess, A. 1998 Direct numerical simulation of forced MHD turbulence at low magnetic Reynolds number. *J. Fluid Mech.* **358**, 299–333.